

As a library, NLM provides access to scientific literature. Inclusion in an NLM database does not imply endorsement of, or agreement with, the contents by NLM or the National Institutes of Health.

Learn more: [PMC Disclaimer](#) | [PMC Copyright Notice](#)

Author Manuscript

Peer reviewed and accepted for publication by a journal



[Life Sci Space Res \(Amst\)](#). Author manuscript; available in PMC: 2019 Feb 1.

Published in final edited form as: [Life Sci Space Res \(Amst\)](#). 2017 Dec 2;16:63–75. doi: [10.1016/j.lssr.2017.11.003](#)

Effects of spaceflight on the immunoglobulin repertoire of unimmunized C57BL/6 mice

[Claire Ward](#)^{1,#}, [Trisha A Rettig](#)^{1,#}, [Savannah Hlavacek](#)¹, [Bailey A Bye](#)¹, [Michael J Pecaut](#)², [Stephen K Chapes](#)¹

[Author information](#) [Article notes](#) [Copyright and License information](#)

PMCID: PMC5826609 NIHMSID: NIHMS928411 PMID: [29475521](#)

The publisher's version of this article is available at [Life Sci Space Res \(Amst\)](#).

Abstract

Spaceflight has been shown to suppress the adaptive immune response, altering the distribution and function of lymphocyte populations. B lymphocytes express highly specific and highly diversified receptors, known as immunoglobulins (Ig), that directly bind and neutralize pathogens. Ig diversity is achieved through the enzymatic splicing of gene segments within the genomic DNA of each B cell in a host. The collection of Ig specificities within a host, or Ig repertoire, has been increasingly characterized in both basic research and clinical settings using high-throughput sequencing technology (HTS). We utilized HTS to test the hypothesis that spaceflight affects the B-cell repertoire. To test this hypothesis, we characterized the impact of spaceflight on the unimmunized Ig repertoire of C57BL/6 mice that were flown aboard the International Space Station (ISS) during the Rodent Research One validation

flight in comparison to ground controls. Individual gene segment usage was similar between ground control and flight animals, however, gene segment combinations and the junctions in which gene segments combine was varied among animals within and between treatment groups. We also found that spontaneous somatic mutations in the IgH and Igk gene loci were not increased. These data suggest that space flight did not affect the B cell repertoire of mice flown and housed on the ISS over a short period of time.

Keywords: Immunoglobulin Gene Use, Next Generation Sequencing, Bioinformatics

1. Introduction

Spaceflight presents a unique set of challenges to the immune system. For example, spaceflight alters T- and B-lymphocyte functions, including recall responses in astronauts aboard the space shuttle and cytokine responses after missions to the international space station (ISS) ([Berry, 1970](#), [Crucian et al., 2013](#), [Crucian et al., 2014b](#), [Grigoriev et al., 1993](#), [Stein and Schluter, 1994](#), [Taylor and Dardano, 1983](#), [Taylor et al., 1986](#), [Rykova et al., 2008](#)). In addition to functional changes, lymphocyte subpopulations are altered. CD8⁺ T-cell numbers were increased during flight while other T-cell subsets were decreased ([Crucian et al., 2013](#)). Similar changes in phenotype also occur in animal and tissue culture systems during spaceflight or ground-based spaceflight analogs such as anti-orthostatic suspension (AOS) ([Chapes et al., 1993](#), [Globus and Morey-Holton, 2016](#), [Crucian et al., 2014a](#), [Nickerson et al., 2003](#), [Sonnenfeld, 2005](#)).

Lymphocyte subpopulations change in response to spaceflight ([Allebban et al., 1994](#), [Chapes et al., 1999a](#), [Gridley et al., 2009](#), [Gridley et al., 2013](#), [Ichiki et al., 1996](#), [Pecaut et al., 2003](#), [Sonnenfeld et al., 1990](#), [Sonnenfeld et al., 1992](#)) and AOS ([Gaignier et al., 2014](#), [Wei et al., 2003](#)). Splenic T- and B-lymphocyte counts were decreased in mice flown on the 13-day mission of the Space Shuttle Endeavor (STS-118) compared to ground controls ([Gridley et al., 2009](#)). In the AOS model, Wei et al. found a reduced number of both T and B lymphocytes in the thymus and spleen of hindlimb unloaded Balb/c mice compared to normal controls ([Wei et al., 2003](#)). Reductions in the mass of lymphoid organs has also been observed ([Armstrong et al., 1993](#), [Baqai et al., 2009](#), [Chapes et al., 1999b](#), [Chapes et al., 1999a](#), [Congdon et al., 1996](#), [Durnova et al., 1976](#), [Gaignier et al., 2014](#), [Grove et al., 1995](#), [Pecaut et al., 2000](#)). Spaceflight altered the phenotype of immune cells in the bone marrow, the lymphoid organ in which hematopoiesis occurs ([Ortega et al., 2009](#)), and AOS reduced the number of bone marrow B-cell progenitors ([Lescale et al., 2015](#)).

While many studies have characterized T-cell response to spaceflight ([Chapes et al., 1999a](#), [Cooper et al., 2001](#), [Grove et al., 1995](#), [Lesnyak et al., 1993](#), [Lesnyak et al., 1996](#), [Nash et al., 1992](#), [Nash and Mastro, 1992](#), [Sanzari et al., 2013](#), [Sonnenfeld et al., 1998](#), [Cogoli et al., 1984](#), [Cogoli-Greuter, 2004](#), [Chang et al., 2012](#), [Gridley et al., 2009](#), [Hwang et al., 2015](#), [Martinez et al., 2015](#), [Tauber et al., 2015](#)), fewer studies have characterized the impact of spaceflight on B-cell populations. The characterization of B-cell receptors, known as immunoglobulins (Igs), is of particular interest due to the (IgH) and light chains, which are encoded on separate loci ([Tonegawa, 1983](#)). The heavy chain locus encodes multiple Variable- (V), Diversity- (D) and Joining- (J) gene segments, while the functionally equivalent κ (Igk) and (Ig)

light chain loci contain only V- and J-gene segments ([Early et al., 1980](#), [Sakano et al., 1979](#)). During early B-cell development in the bone marrow, B cells undergo recombination of heavy and light chain Ig loci, in which only one of each V(D)J-gene segment is selected for Ig use ([Hozumi and Tonegawa, 1976](#), [Tonegawa, 1983](#)). Random and palindromic nucleotide insertion at splice sites adds to Ig diversity ([Alt et al., 1984](#), [Gilfillan et al., 1993](#), [Komori et al., 1993](#)).

In the Ig molecule, complementarity determining regions (CDR) confer binding specificity. CDR1 and CDR2 are encoded entirely within the V-gene segment, while CDR3 contains a portion of the 3' end of the V-gene segment, the entire D-gene segment, and a portion of the 5' end of the J gene segment ([Kabat et al., 1979](#), [Tonegawa, 1983](#), [Xu and Davis, 2000](#)). As a result of somatic recombination, B cells collectively express individual Igs that theoretically can bind virtually any pathogen.

An individual's Ig repertoire can be characterized using high-throughput sequencing (HTS) using either genomic DNA or messenger RNA sequences isolated from B-cell populations ([Georgiou et al., 2014](#), [Rettig et al., 2017](#), [Wardemann, 2017](#)). B cells will clonally expand after antigen-Ig receptor engagement, resulting in a higher portion of target-specific Ig receptors within the B-cell population. There have been a number of HTS-based Ig repertoire studies in human disease, ranging from infectious disease ([Ademokun et al., 2011](#), [Khurana et al., 2016](#), [Lee et al., 2016](#), [Parameswaran et al., 2013](#)), autoimmunity ([Tan et al., 2014](#), [Tan et al., 2016](#), [Zuckerman et al., 2010](#)), and cancer ([Bashford-Rogers et al., 2016](#), [Jiang et al., 2015](#), [Logan et al., 2011](#), [Montesinos-Rongen et al., 2014](#), [Tschumper et al., 2012](#)). Greiff, et al. developed a profiling framework using the Ig repertoire as an indicator of an individual's immunological status ([Greiff et al., 2015](#)).

Some have explored the impact of spaceflight on Ig repertoires. *In vitro* challenge of human B cells during spaceflight resulted in lower concentrations of secreted Ig ([Fitzgerald et al., 2009](#)). There was no significant difference in pre- and post-flight Ig levels in peripheral blood of astronauts who flew aboard the ISS ([Stowe et al., 1999](#), [Rykova et al., 2008](#), [Voss, 1984](#)). These samples, however, were not taken after challenge with a specific antigen. Rats immunized intraperitoneally with sheep red blood cells prior to spaceflight produced significantly less serum IgG compared to immunized ground control animals ([Lesnyak et al., 1993](#)).

Although some have explored Ig gene segment changes in the context of spaceflight or model analogs ([Boxio et al., 2005](#), [Bascove et al., 2009](#), [Bascove et al., 2011](#), [Huin-Schohn et al., 2013](#)), little has been done to characterize the impact of spaceflight on the Ig repertoire in mice. Given that changes in B cells and Ig concentrations occur during spaceflight conditions, we tested the hypothesis that spaceflight alters the Ig repertoire of mice flown on the ISS. We examined individual Ig gene segment usage, gene segment combinations, CDR3 composition, and frame work and CDR mutations in 35-week-old, unimmunized, female C57BL/6Tac mice flown aboard the ISS using high throughput sequencing.

2. Materials and Methods

2.1 Tissue Samples

RNA samples were provided by the NASA Ames Research Center. RNA was extracted from the spleen and liver of 35-week-old female C57BL/6Tac mice that were either housed in the ISS environmental simulator (ground control, n=5), or flown aboard the ISS via SpaceX-4 (n=5). Tissues from flight animals were collected on board the ISS 21–22 days post-launch in flight animals while tissues from ground control animals were processed similarly on a four-day delay. Upon collection, spleens and livers were stored at 4°C in RNAlater (Life Technologies, Carlsbad, CA) for at least 24 hours and then stored at –80°C. RNA extraction was performed according to manufacturer's instructions with the RNeasy mini column (QIAGEN, Hilden, Germany) and stored at –80°C. This was a secondary science experiment and the dissection and timing of the experiment were dictated by the primary validation experiment. Animal care and experimental procedures were approved by the Institutional Animal Care and Use Committee at the NASA Ames Research Center.

2.2 Illumina MiSeq Sequencing

RNA samples were subjected to Illumina MiSeq sequencing at the Kansas State University Integrated Genomics Facility as previously outlined in Rettig *et al* ([Rettig et al., 2017](#)). Briefly, sequencing was performed using the standard MiSeq protocol which includes oligo-dT-bead selection and reverse transcription of mRNA to cDNA. Ig-specific primer amplification was not utilized. Additionally, fragmentation was limited to one minute to reduce fragmentation and maintain longer reads. Illumina MiSeq with paired reads of 300 base pairs was performed on size selected (275–800 nt) total RNA isolated from the liver and spleen of three ground control and three flight animals based on highest RIN values (Spleen RIN: 5.9–8.9, Liver RIN: 6.2–7.8) (Ground animals: G1, G2, G3; Flight animals: F1, F2, F3). Illumina MiSeq data from both spleen and liver are available by NASA GeneLab (<https://genelab.nasa.gov> , GLDS-ID Pending).

2.3 Bioinformatic Workflow

Illumina MiSeq sequencing reads were processed as described previously ([Rettig et al., 2017](#)). Briefly, FASTQ files were imported into CLC Genomics Workbench v9.5.1 (<https://www.qiagenbioinformatics.com/>) and were quality trimmed and filtered to remove sequences less than 40 nt in length to prevent false V-gene segment assignment. Paired-end sequences and overlapping-paired (merged) sequences were mapped to both V-gene segment references obtained from the ImMunoGeneTics (IMGT) database (251 IgH segments, 135 Igk segments), and to entire IgH and Igk loci obtained from NCBI ([NC_000078.6](#), 113258768 to 116009954, and [NC_000072.6](#), 67555636 to 70726754, respectively). Mapped sequencing reads were submitted to the IMGT HighV-Quest tool for characterization of

functionality and junctional analysis. Only one sequence per sequencing cluster was retained for further analysis as outlined in Rettig *et al* ([Rettig et al., 2017](#)). Briefly, per sequencing organization ID, the read with the most information is saved for further analysis. Antibody sequences can differ by as little as a single nucleotide and without a unique barcoding step during amplification, removing similar, but not identical sequences, could limit the breadth of the repertoire sampled. Due to this, no further filtering was performed on sequences. A motif search was performed in CLC on IgH sequences that were identified by IMGT as productive to determine their respective constant regions.

2.4 Gene Segment Usage

Sequencing reads were analyzed using the IMGT HighV-Quest tool ([Alamyar et al., 2012](#)). V-gene segment usage was characterized as either productive or unknown functionality, where a read was considered productive if it was in frame and did not contain a premature stop codon as defined by IMGT. Sequences that did not fit the C-xx-W motif in non-class switched H-CDR3 or C-xx-F in κ -CDR3 were assigned an unknown functionality. D- and J-gene segment, and constant region usage was assessed in productive reads only. All gene segments considered functional by IMGT (includes open reading frames and gene segments without full NCBI mapping) were included in this analysis. Reads assigned to multiple C57BL/6 V-gene segments were tabulated using a weighted distribution. Reads containing only one possible V-gene segment were assigned a count of one. Reads containing two possible V-gene segments were assigned a count of 0.5 for each potential V-gene segment. Reads containing more than two potential V-gene segments were excluded from V-gene analysis. Multiple V-gene segment assignments likely resulted from reads containing less than a full V-gene segment as a result of random hexamer priming. Reads assigned to a single non-C57BL/6 D/J-gene segments or multiple C57BL/6 D/J-gene segments were reclassified as undetermined and kept for analysis. J-gene segments in which less than six nucleotides were identified were also classified as undetermined. Percent of repertoire was determined for each individual animal by dividing the number of sequencing reads for each gene segment by the total number of sequencing reads mapped to all gene segments.

2.5 Gene Segment Combination & CDR3 Analysis

Reads assigned to non-C57BL/6 V-gene segments or multiple C57BL/6 V-gene segments were removed from our V(D)J combination analyses. V(D)J combination analyses were performed on productive sequencing reads and visualized through the use of bubble charts (Microsoft Excel) and/or circos graphs from Circos Online ([Krzywinski et al., 2009](#)). Percent repertoire was used to detail individual bubble charts and the average of percent repertoire was used when combining mice from each treatment group for V(D)J bubble chart analysis. CDR3 amino acid sequence was presented as percent of repertoire as described above and by a highest to lowest ranking of abundance.

CDR3 nucleotide alignments were created using the MAFFT multiple sequence alignment program ([Katoh et al., 2002](#)). A V-D-J-gene segment combination was selected from the top ten percent most-represented gene segments across all

individuals for both heavy and light chain. From each individual group, unique nucleotide sequences were isolated and aligned to their respective germline sequences provided by IMGT. Individual alignments were then stacked within their treatment groups and germline gaps were adjusted for consistency across treatment groups.

2.6 Complementarity Determining and Framework Region Mutation Analysis

Nucleotide substitution mutation data for complementarity determining and framework regions for IgH and Igk were obtained from the IMGT HighV-Quest tool. Any mutations involving degenerate bases were removed. Nucleotide range (in base pairs), number of reads containing at least one mutation, total number of substitution mutations, and number of mutations per base pair position were determined for each region. Comparative values for each combination of region, Ig location, and treatment group were determined by calculating the average of values contained in each combination's respective replicates (n=3).

2.7 Statistical Analysis and Representation of Data

All statistical analyses were performed in GraphPad (version 6.0). Dot plots and bar graphs were generated in GraphPad using mean values and standard deviation. Heat maps of gene segment usage were generated in Microsoft Excel.

3 Results

3.1 V-Gene Segment Usage

B cells originate in the bone marrow from hematopoietic precursors, traffic through the periphery and enter the spleen where they are further selected and mature ([Loder et al., 1999](#)). To view a snapshot of the impact that spaceflight has on the splenic Ig repertoire of unimmunized mice, we sequenced total splenic RNA isolated from three ground control animals and three animals flown aboard the ISS. We assessed the composition of individual IgH and Igk sequences. In spleen, between 104,135 and 149,675 IgH, and between 103,841 and 175,406 Igk sequencing reads of productive or unknown functionality were detected in ground animals, while between 66,909 and 181,703 IgH, and between 81,889 and 107,928 Igk were detected in flight animals ([Table 1](#)).

Table 1.

Spleen Sequencing Read Counts in Ground (G) and Flight (F) Mice

	G1	G2	G3	F1	F2	F3
Raw Reads ^{a, b}	51.4 M	45.2 M	43.5 M	40.5 M	48.4 M	55.8 M
Cleaned ^{a, c}	13.2 M	31.4 M	30.9 M	14.6 M	13.0 M	14.1 M
IgH IMGT ^{d, e}	124,102	104,135	149,675	85,802	66,909	181,703
Igk IMGT ^{d, e}	175,406	140,963	103,841	107,851	81,889	107,928

[Open in a new tab](#)^aM=Million^bRaw reads reflect unfiltered FASTQ files imported from the Illumina MiSeq personal sequencing system.^cCleaned reads were quality trimmed to remove the first 12 base pairs, reads with a Phred score under 20, and sequences less than 40 nt in length.^dMapped Ig Sequencing reads of productive or unknown functionality were obtained from the IMGT HighV-Quest tool.^eThere is no statistical significance by student's t-test in the number of reads mapped to IgH ($p=0.7215$) and Igk ($p=0.1424$).

The V-gene segment contributes to the combinatorial diversity of the Ig repertoire in part due to the large number of possible V-gene segments that could be selected within an individual B cell. Among the six study animals 133 VH- and 108 V κ -gene segments were detected. Overall, the frequency of highly abundant V-gene segments and less frequently identified V-gene segments were similar between treatment groups ([Supplementary Figure 1](#)). Despite a general similarity, a pairwise comparison of animals within treatment groups showed low-to-moderate levels of VH-gene segment correlation (Ground R^2 : 0.356–0.695, p -values: <0.001 ; Flight R^2 : 0.101–0.360, p -values:0.0001– <0.0001) that demonstrates that there is animal-to-animal variation ([Table 2](#)). A stronger correlation was seen in V κ -gene segments (Ground R^2 : 0.660–0.738, p -values <0.0001 ; Flight R^2 : 0.465–0.606, p -values <0.0001) ([Table 2](#)). When comparing the average abundance of V-gene segments from ground and flight animals an R^2 of 0.592 was observed in VH ($p=<0.0001$) and 0.810 was observed in V κ ($p=<0.0001$) ([Table 2](#)).

Table 2.

Comparison of Flight and Ground V-Gene Segment Usage

Comparison	VH R ²	Vκ R ²
G1 v G2	0.620	0.660
G2 v G3	0.356	0.738
G1 v G3	0.695	0.678
F1 v F2	0.101	0.465
F2 v F3	0.225	0.516
F1 v F3	0.360	0.606
Mean G v F	0.592	0.810

[Open in a new tab](#)

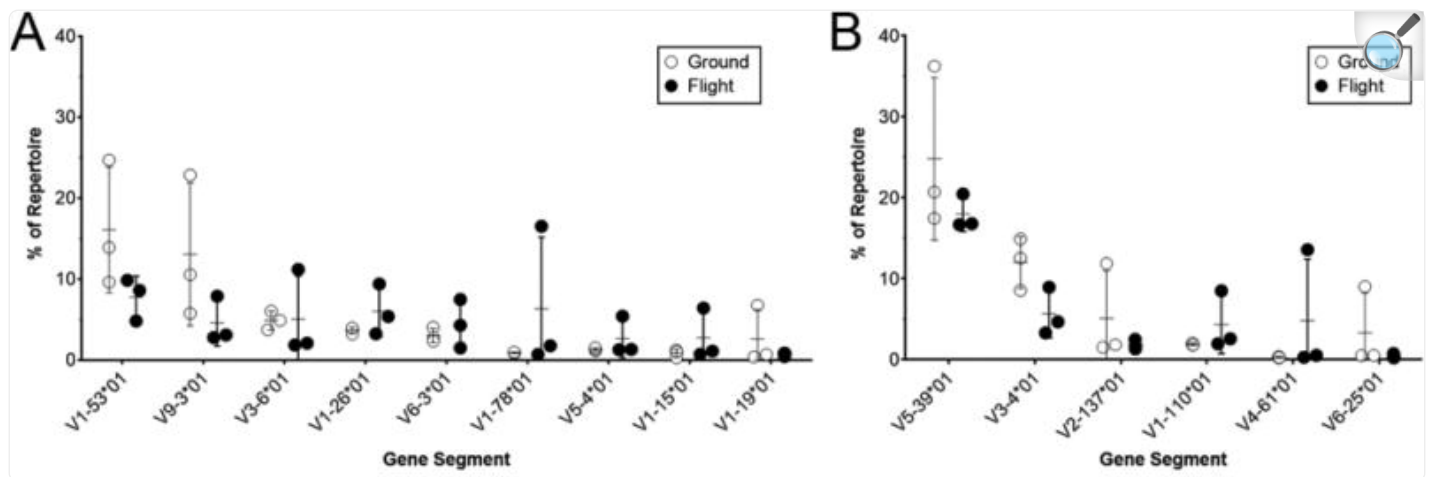
Pairwise linear regressions of VH- and Vκ-gene segment usage were performed among ground control (G) and flight (F) animals. A linear regression was performed on the mean-average V gene segment of ground and flight treatment groups.

^aAll comparison groups were correlated ($p \leq 0.0001$)

When comparing VH-gene usage among all animals, nine gene segments represented over five percent of the repertoire in at least one animal ([Figure 1A](#)). No one gene segment was found at over the five percent level in all six animals.

V1-53 was found in over five percent in five animals, V9-3 was over five percent in four animals, V1-26 and V3-6 in two animals, and the remaining (V1-78, V6-3, V5-4, V1-15, V1-19) were found at high levels in only one animal.

Figure 1. Expression of Top V-Gene Segments.



[Open in a new tab](#)

(A) VH- and (B) Vκ-gene segment usage for gene segments representing over five-percent of the repertoire in at least one animal within ground and flight treatment groups. No significant difference in individual gene segment usage was detected between ground control and flight treatment groups (Student's *t*-test, $0.1534 < p\text{-value} < 0.9609$). Significant differences between gene segment usage of combined ground and flight animals were found. In IgH, V1-53 was more abundant than many of the top V-gene segments (V1-78, V5-4, V1-15, V1-19); (Student's *t*-test, all $p < 0.05$). In Igκ, V5-39 was more abundant than many of the top V-gene segments (V3-4, V2-137, V1-110, V4-61, V6-25); (Student's *t*-test, all $p < 0.05$).

Within Vκ, six gene segments represented over five percent of the repertoire in at least one animal ([Figure 1B](#)). The most abundant gene segment, V5–39 comprised over 16 percent of Vκ usage in all six animals. No other Vκ represented over five percent of the repertoire in all six animals. One gene segment, V3–4, was found at over five percent of the repertoire in four animals (G1, G2, G3, F3). The remaining four gene segments (V2–137, V1-110, V4–61, and V6–25) were found at greater than five percent in only one animal. There was no statistical difference in top VH- or Vκ-gene segment usage between ground and flight animals (student's *t*-test, $p = 0.6478\text{--}0.9609$).

We also attempted to assess the antibody repertoire in the liver because of its role in fetal B-cell development. Only 592 to 1,429 Igκ sequencing reads were detected in ground control animals and 425 to 543 Igκ sequencing reads were detected in flight animals ([Table 3](#)). We did not characterize the heavy chain in the liver due to the low number of IgH sequencing reads that we detected. We assessed Vκ-gene segments that represented over five percent of the repertoire in the spleen or liver and found 11 gene segments. Only one gene segment, V5–39, was found in the top five across both

tissues ([Figure 2](#)). V3–4 was found in the top five for all animals and tissues except flight mouse two’s liver sample, where it was ranked tenth. Overall, the average usage of these top Vκ-gene segments showed low to modest correlation between liver and spleen in ground animals ($R^2= 0.4081, p<0.0001$) and flight animals ($R^2= 0.2727, p<0.0001$). Analysis of statistical differences between individual Vκ-gene segments representing over five percent of the repertoire was not undertaken due to low read counts in the liver datasets.

Table 3.

Vκ Liver Sequencing Read Counts in Ground (G) and Flight (F) Mice

	G1	G2	G3	F1	F2	F3
Raw Reads ^{a, b}	43.9 M	42.9 M	38.4 M	49.2 M	48.3 M	39.7 M
Cleaned ^{a, c}	18.8 M	35 M	31.5 M	24.7 M	18.2 M	19.4 M
Igκ IMGT ^{d, e}	1429	1267	592	543	425	438

[Open in a new tab](#)

^aM=Million

^bRaw reads reflect unfiltered FASTQ files imported from the Illumina MiSeq personal sequencing system.

^cCleaned reads were quality trimmed to remove the first 12 base pairs, reads with a Phred score under 20, and sequences less than 40 nt in length.

^dMapped Ig Sequencing reads of productive or unknown functionality were obtained from the IMGT HighV-Quest tool.

Figure 2. Expression of Top-V κ Gene Segments from Spleen and Liver.

	LG1	LG2	LG3	LF1	LF2	LF3		SG1	SG2	SG3	SF1	SF2	SF3
V5-39*01	4	1	4	1	2	2	V5-39*01	1	1	1	1	1	1
V3-4*01	5	2	2	5	10	5	V3-4*01	2	2	2	5	5	2
V1-110*01	12	5	10	14	5	8	V1-110*01	9	10	11	14	9	3
V2-137*01	16	9	3	11	20	13	V2-137*01	16	9	3	8	14	19
V3-2*01	2	3	31	40	4	15	V3-2*01	19	8	21	20	8	14
V6-20*01	3	14	44	20	36	15	V6-20*01	13	37	32	15	29	23
V4-91*01	52	30	58	34	36	3	V4-91*01	47	40	33	32	18	7
V4-61*01	47	20	76	62	3	19	V4-61*01	60	48	57	55	2	37
V4-81*01	8	4	1	1	1	1	V4-81*01	82	81	81	82	83	78
V6-25*01	6	90	58	94	70	76	V6-25*01	3	41	38	28	59	54
V6-14*01	1	78	76	76	87	76	V6-14*01	50	71	63	73	57	69

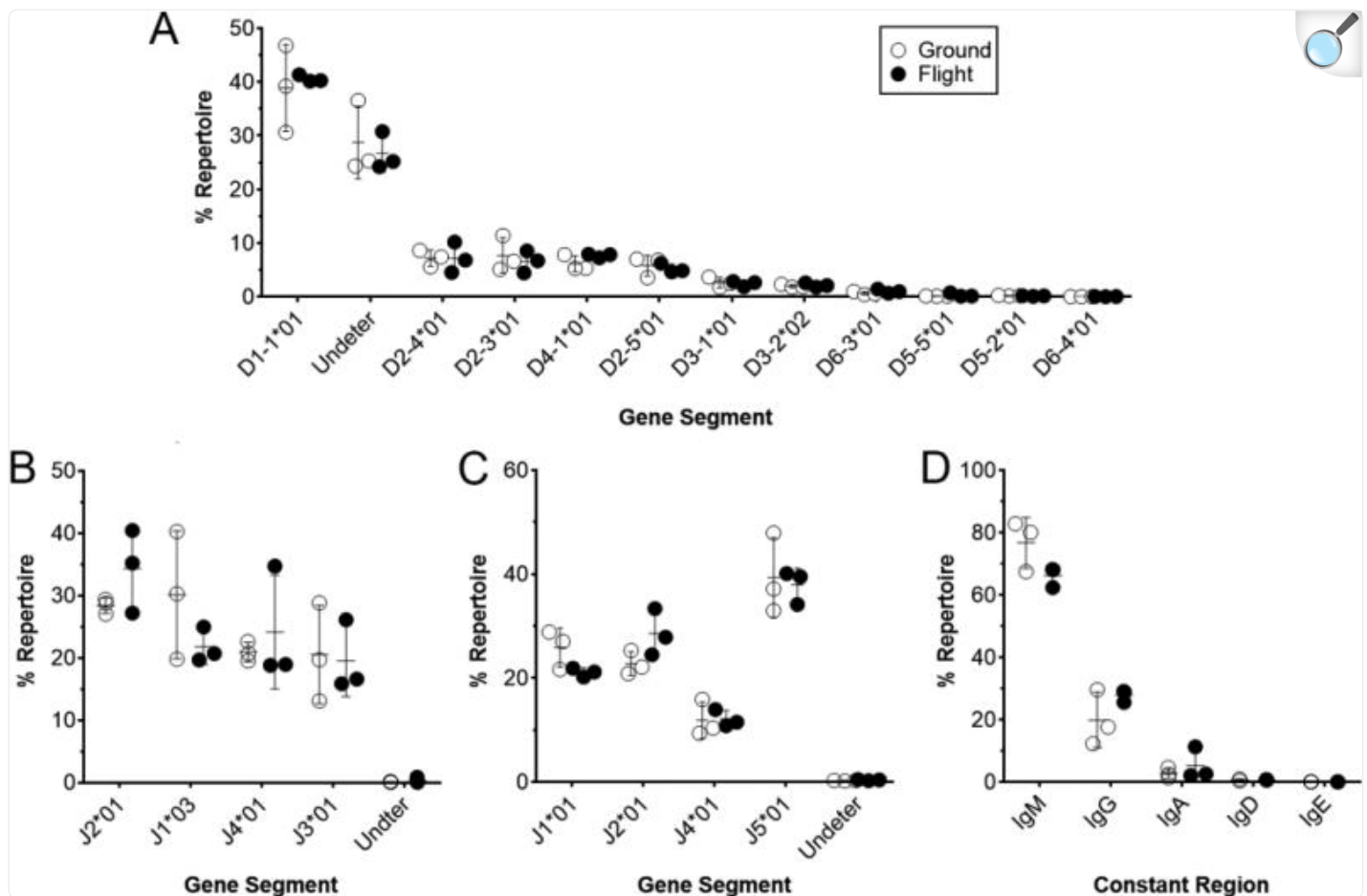
[Open in a new tab](#)

V κ -gene segment usage for gene segments representing over five-percent of the repertoire in at least one animal from the liver or spleen of ground or flight animals are presented by rank. Liver ground (LG) and liver flight (LF) rankings are shown to the left and spleen ground (SG) and spleen flight (SF) rankings are shown to the right. V-gene segments are listed most frequent to least frequent. Dark red indicates higher rank moving to blue, lower percent rank.

3.2 D- and J-Gene Segment & Constant Region Usage

Heavy chain Ig diversity is also achieved by using, modifying and splicing of D-and J-gene segments. To determine if space flight affected these processes we also assessed D- and J-gene usage. The most commonly detected D-gene segment in both ground control and flight animals was D1-1, comprising between 30.6% to 46.8% of the repertoire ([Figure 3A](#), [Supplemental Figure 2A](#)). D2-4, D2-3, D4-1, and D2-5 were detected at similar levels among ground control and flight animals between 3.56% and 11.39% of the repertoire. D3-1, D3-2, D6-3, D5-5, and D5-2, and D6-4 were detected the least often with levels between 3.6% and >0.003% of the repertoire. Because of extensive modification of D-gene segments during IgH rearrangement, D-gene segments were unable to be determined for between 24.4% and 36.6% of the repertoire for all animals. There was no statistical difference in D-gene segment usage between ground and flight animals (student's t-test, $p=0.1542-0.9840$). D-gene segment usage was highly correlated between ground and flight animals (linear regression, $R^2=0.9935$, $p<0.0001$).

Figure 3. Expression of D and J-Gene segments and IgH Constant Region Usage.



[Open in a new tab](#)

(A) D-gene segment, (B) JH-gene segment, (C) Jκ-gene segment, and (D) IgH constant region usage in animals within ground and flight treatment groups are presented as percent of repertoire. No significant difference in individual gene segment usage was detected between ground control and flight treatment groups (Student's *t*-test, D: $0.1542 < p\text{-value} < 0.9840$, JH: $0.2060 < p\text{-value} < 0.8662$, IgH Constant Region: $0.1075 < p\text{-value} < 0.8277$, Jκ: $0.0977 < p\text{-value} < 0.9262$). D1-1 was used at a significantly higher rate than all other D-gene segments (Student's *t*-test, all significant $p < 0.05$). No significant differences between JH-gene segment usage were found (Student's *t*-test, all $p < 0.05$). In Igκ, significant differences in expression were found between all gene segments except between J1 and J2 (Student's *t*-test, all significant $p < 0.05$).

Additional Ig variability is gained from the inclusion of different J-gene segments. Within IgH, the distribution of J-gene segment usage was less uniform than D-gene segment usage in both ground and flight animals. There was no consensus

on the most abundantly expressed gene segment as each of the four JH-gene segments was the most abundant segment in at least one ground or flight animal ([Figure 3B](#), [Supplemental Figure 2B](#)). While there was no consensus use of a particular J-gene segment, usage of any J-gene segment was between 13% and 40%, showing that usage is relatively uniform. Student's *t*-tests were performed to determine whether differences in individual gene segment usage were significant. No significant differences were found between ground and flight animals (student's *t*-test, $p=0.2060-0.8662$). As the most abundant J κ -gene segment, J5, comprises between 32.6% and 47.9% of the repertoire, and is the most abundant gene segment all study animals ([Figure 3C](#), [Supplemental Figure 2C](#)). Interestingly J1 ranked second most abundant in all ground animals while it ranked third in all flight animals. There were no statistical differences in individual JH- or J κ -gene segment usage between ground control and flight animals (Student's *t*-test, $p=0.0977-0.9262$). Linear regression revealed correlation between JH usage of ground and flight animals for Ig κ ($R^2=0.9928$, $p=0.0076$) and IgH ($R^2=0.8147$, $p=0.0360$).

Ig isotype composition can provide insight into the developmental stage of B cells. Because animals in this experiment were specific-pathogen free, it is unsurprising that IgM predominated with between 62.38% and 82.81% of the repertoire ([Figure 3D](#), [Supplemental Figure 2D](#)). IgG was the second most prominent isotype which trended towards a higher percentage of the repertoire in flight animals although the difference was not statistically significant (Student's *t*-test, $p=0.2150$). Except for a relatively high expression of IgA in flight mouse two, IgA was detected in between 1.43% and 4.58% of the repertoire, IgD and IgE were detected less than one percent in all animals. There were no statistical differences in Ig isotype frequency between ground and flight animals (Student's *t*-test, $p=0.1075-0.8277$). There was a high correlation between ground and flight constant region usage (linear regression, $R^2=0.9734$, $p=0.0019$).

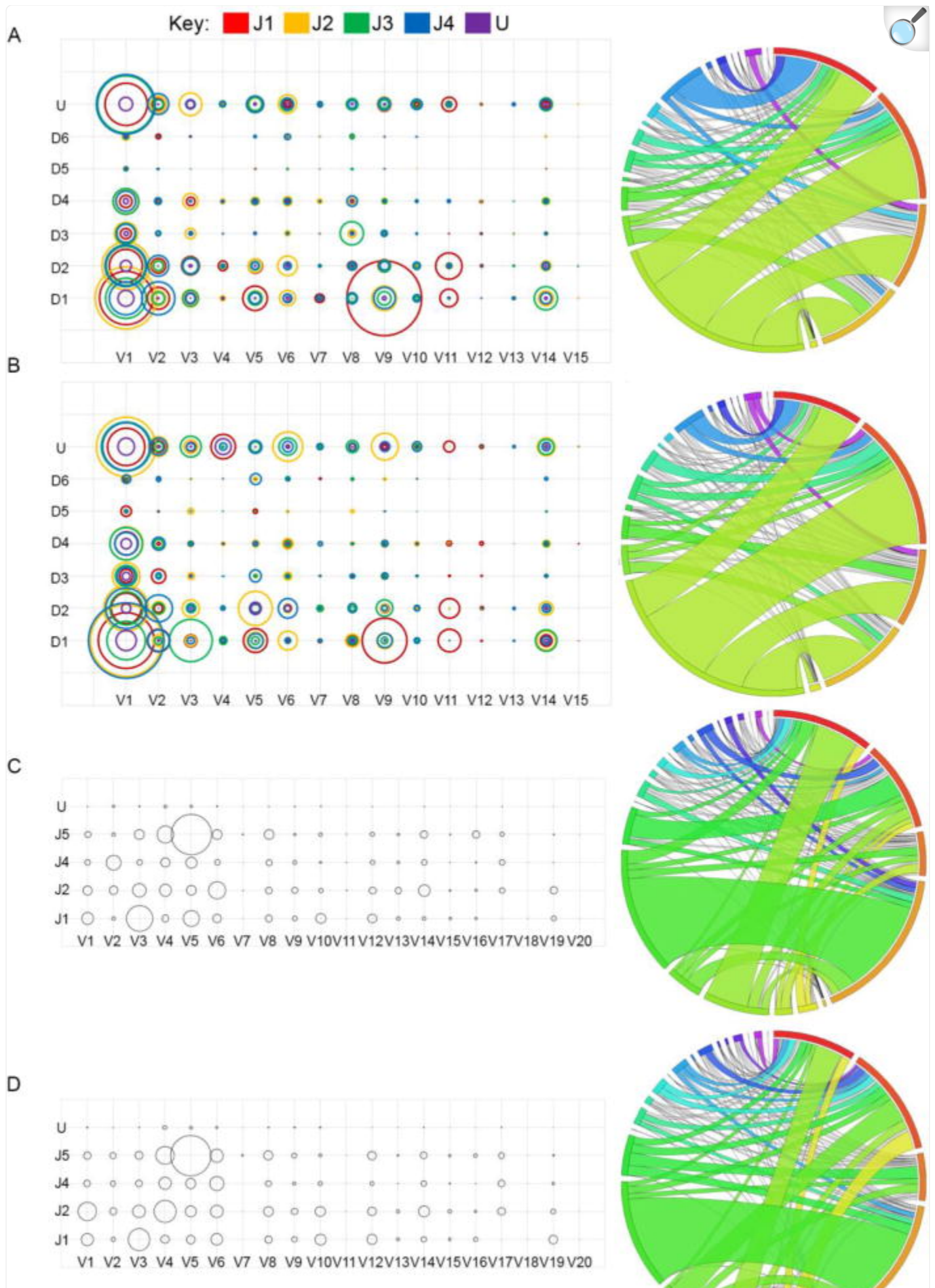
3.3 V(D)J Combinations

V(D)J family combinations were examined as another way to determine if recombination of Ig gene segments was affected by spaceflight. We visualized V(D)J-gene segment combinations using both bubble charts and circos plots for both IgH and Ig κ . IgH showed more variation between ground control and flight animals compared to Ig κ when looking at the most common gene family combinations. Circos plots allowed us to examine top V-gene families, J-gene segments, and V/J pairing frequency in both IgH and Ig κ .

For ease of display, we first grouped together all V-gene segments into their respective family. D- and J-gene segments remained as individuals. V1 was the most common IgH gene family used in all mice comprising, on average 51% of the V-gene family use in ground animals and, on average, 57% of the repertoire in flight animals ([Figure 4A-B](#), [Supplemental Figure 3A-F](#)). In ground-treatment animals, V9 was the second most common gene family in ground mouse one and ground mouse two, while V2 was the second most common gene family in ground mouse three ([Figure 4A](#), [Supplemental Figure 3A-C](#)). In flight animals, the second most common V-gene family used was unique among the three animals (flight one: V3, flight two: V2, and flight three: V9) ([Figure 3B](#), [Supplemental Figure 4D-F](#)). The third most common V-gene family was also unique among the ground treatment animals being V2, V3, and V9 for ground

mouse one, ground mouse two, and ground mouse three respectively ([Figure 4A](#), [Supplemental Figure 3A–C](#)). V5 was the third most common family in flight mouse one, V9 in flight mouse two, and V2 in flight mouse three ([Figure 4B](#), [Supplemental 3D–F](#)).

Figure 4. Gene Segment Combinations in Ground Control and Flight Animals.





[Open in a new tab](#)

(A, B) Average IgH V/D/J combinations (bubble chart) and the V/J combinations (Circos plot) for ground treatment (A) animals and (B) flight animals. For bubble charts, V-gene family is represented along the x-axis, the D-gene segment is represented along the y-axis, and the J-gene segment is represented by a specific color. The size of the bubble corresponds to the average percent repertoire of the specific gene combination. Circos plots are read clockwise starting at the 12 o'clock position with J1 (red), J2, J3, J4, U, V1 (lime green), V2, V3, V4, V5, V6, V7, V8 (light blue), V9, V10, V11, V12, V13, V14, and V15 (sliver, no color). (C,D) Average Igk V/J combinations for ground treatment (C) animals and (D) flight animals. For bubble charts, V-gene family is represented along the x-axis and J-gene segment is represented along the x axis. The size of the bubble corresponds to the average percent repertoire of the specific gene combination. Circos plots are read clockwise starting at the 12 o'clock position with J1 (red), J2, J4, J5, U, V1 (yellow), V2, V3, V4, V5, V6, V7 (sliver, no color), V8, V9, V10, V11, V12, V13, V14, V15, V16, V17, V18, V19 (light purple).

We found that the most common V/D/J combinations were correlated with the most frequently used gene families or segments within the repertoire. When averaging among repertoires, the most common IgH combination in ground-treatment animals was V9/D1/J1 (8.66%), though this combination was only in the top five most frequent combinations in ground mouse one and ground mouse two. The most common average combination in flight-treatment animals was V1/D1/J4 (8.35%), though this combination was only detected in the five most common combinations for one animal ([Figure 4A–B](#), [Supplemental Figure 4A–B](#)). The V1/D1/J2 combination was shared among the top five gene family combinations in all mice; representing 5.94% of the repertoire in ground-treatment animals and 7.73% in the flight-treatment animals ([Supplemental Figure 4A–B](#)). A notable difference between ground and flight treatment groups was the usage of the V9-gene family. This family represented the top average VH-gene family used in the ground-treatment animals as well as the top combination in ground mouse one and ground mouse two ([Figure 4A](#), [Supplemental Figure 4A](#)), but only appeared once as the top gene family combination used for flight-treatment animals ([Figure 4B](#), [Supplemental Figure 4B](#)).

We also examined the top five V/J pairing frequencies for IgH ([Figure 4A–B](#), [Supplemental Figure 3A–F](#), [Supplemental Figure 4C–D](#)). For ground animals, there were six unique pairings represented. The V1 family was used for four of the six unique V/J pairings compiled. V9 and V2 were also used. Of the six unique pairings, four were shared among all three mice (V1/J1, V1/J2, V1/J3, and V1/J4). One was shared among two mice (V9/J1), and one (V2/J4) was found only in ground mouse three's five most common combinations ([Figure 4A](#), [Supplemental Figure 3A–C](#), [Supplemental Figure 4C](#)). For flight animals, seven unique pairings were found in the five most common pairs. V1 was again the overwhelmingly most common V family with four of the seven unique pairings including it. V3, V2, and V9 were all

used by a single animal. Of the seven unique pairs, four were shared among all three mice (V1/J1, V1/J2, V1/J3, and V1/J4). These pairings were also among the most common in the ground-treatment group. Three (V3/J3, V2/J4, V9/J1) were found in a single mouse's five most common pairings ([Figure 4B](#), [Supplemental Figure 3D–F](#), [Supplemental Figure 4D](#)).

We undertook similar analysis for Igk sequences ([Figure 4C–D](#), [Supplemental Figure 3G–L](#), [Supplemental Figure 4E–F](#)). The most common V κ -gene family expressed in all mice was V5, representing over one-fifth of the repertoire. The second most common V κ -gene family in ground animals was V3 while in flight animals it was V6 or V4 ([Figure 4C–D](#), [Supplemental Figure 3G–L](#), [Supplemental Figure 4E–F](#)). The third most represented V κ -gene families was V6 for ground mouse one, and V4 for ground mouse two, and V2 for mouse three ([Figure 4C](#), [Supplemental Figure 4G–I](#)). In flight animals, the third most common V κ -gene family was V4 for flight mouse one, and V3 for flight mouse two and three ([Figure 4D](#), [Supplemental Figure 4J–L](#)).

Unlike IgH, Igk expressed more variety in V/J pairing variety. In Igk there were five pairings in ground animals (V2/J4, V3/J2, V3/J5, V5/J1, V6/J2) that were not shared with the top five flight-animal pairings ([Figure 4C–D](#), [Supplemental Figure 3G–L](#), [Supplemental Figure 4E–F](#)). There were also four pairings (V1/J2, V4/J2, V6/J1, V6/J4) found in flight animals not found in the top five ground-animal pairings ([Figure 4C–D](#), [Supplemental Figure 3G–L](#), [Supplemental Figure 4E–F](#)).

The correlation of the average percent of repertoire for V/J combinations between ground and flight animals was higher in Igk, with a R^2 of 0.8795 ($p < 0.0001$), whereas IgH had a R^2 of 0.3296 ($p < 0.0001$) (linear regression). V/J combination usage among animals within each treatment group also showed stronger correlation within Igk than IgH in both ground and flight treatment groups ([Table 4](#)).

Table 4.

V-J Linear Regression Analyses

Comparison	IgH R ²	Igκ R ²
G1 vs G2 ^a	0.534	0.750
G2 vs G3 ^a	0.124	0.7209
G1 vs G3 ^a	0.256	0.657
F1 vs F2 ^b	0.010	0.539
F2 vs F3 ^a	0.067	0.598
F1 vs F3 ^a	0.103	0.738
G vs F AVG ^a	0.330	0.880

[Open in a new tab](#)

Pairwise linear regression analyses of IgH and Igκ V/J-gene segment combination abundances were performed among grounds control (G) and flight (F) animals. A linear regression was performed on the mean-average V/J-gene segment combination abundances of ground and flight treatment groups.

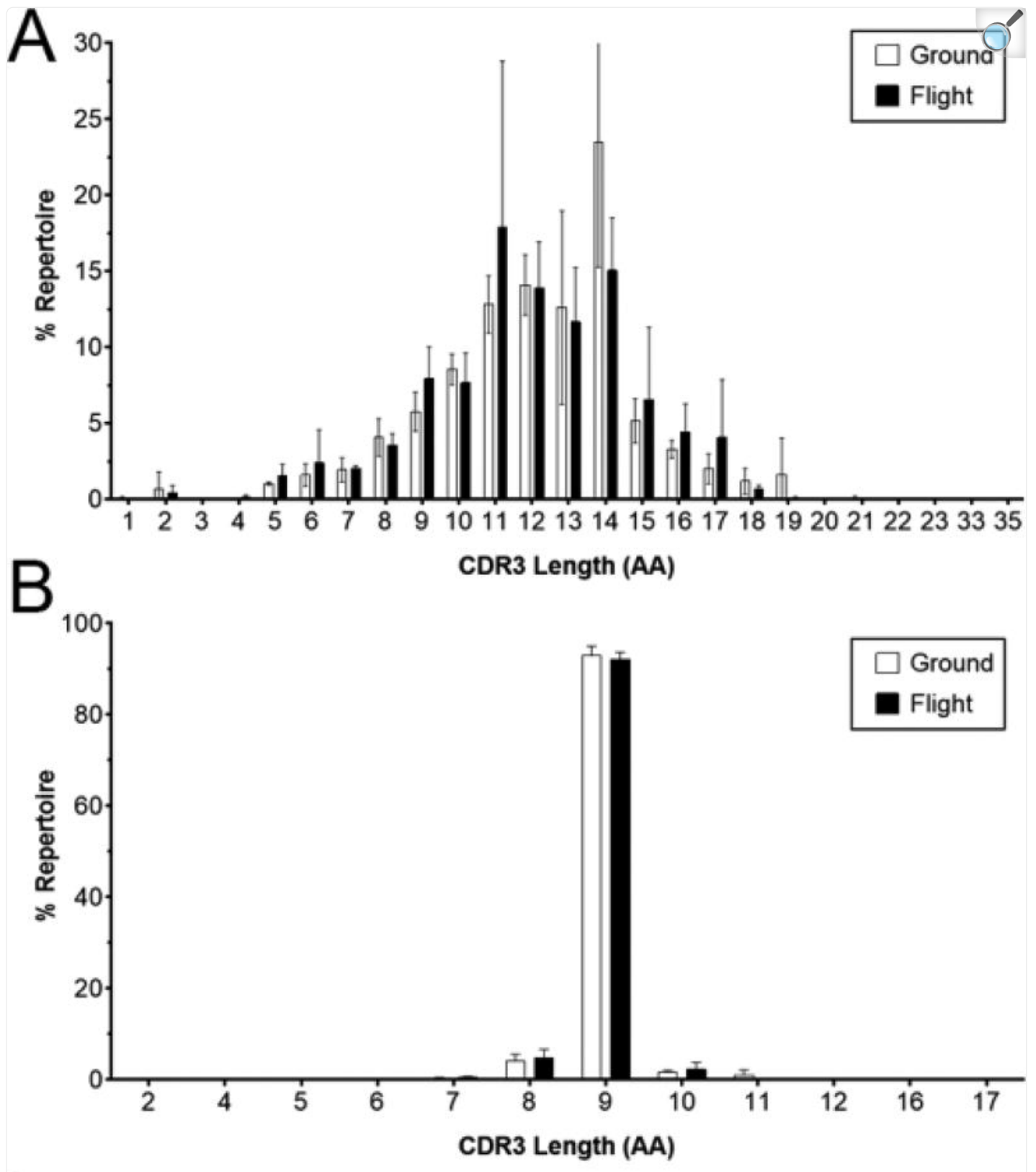
^aComparison group was correlated ($p < 0.0001$)

^bComparison group was correlated for IgH ($p = 0.035$) and Igκ ($p < 0.0001$)

3.4 CDR3

CDR3 is important for conferring diversity in Ig specificity. Therefore, we assessed whether spaceflight had an impact on several properties of CDR3 because changes in CDR3 could affect host ability to respond to antigen. We found that CDR3 length in IgH was highly varied. The length ranged from one amino acid to 35 ([Figure 5A](#)). The average CDR3 lengths for all the ground control animals was 12 ± 0 . The average CDR3 lengths for flight animals was also 12 ± 1 . The CDR3 lengths were not normally distributed in the flight or ground animals (flight $p < 0.0001$, ground $p = 0.0128$) with the majority of CDR3 lengths falling between 11 and 14 AAs. We also examined the heavy-chain CDR3 length by isotype ([Table 5](#)) and by treatment group. We found no significant difference by treatment group or by isotype (two-way ANOVA, interaction $p = 0.8141$, isotype $p = 0.4589$, treatment $p = 0.6225$).

Figure 5. CDR3 Length in IgH and Igk sequences.



(A) IgH and (B) Igκ CDR3 amino acid length of ground control and flight animals as mean-average with standard deviation.

Table 5.

CDR3 Length by Isotype

CDR3 Amino Acid Length						
Isotype	G1	G2	G3	F1	F2	F3
IgA	10	13	12	13	11	12
IgD	11	12	12	12	12	12
IgE	14	11	12	14	11	15
IgG	12	12	13	13	11	12
IgM	12	12	12	12	11	12

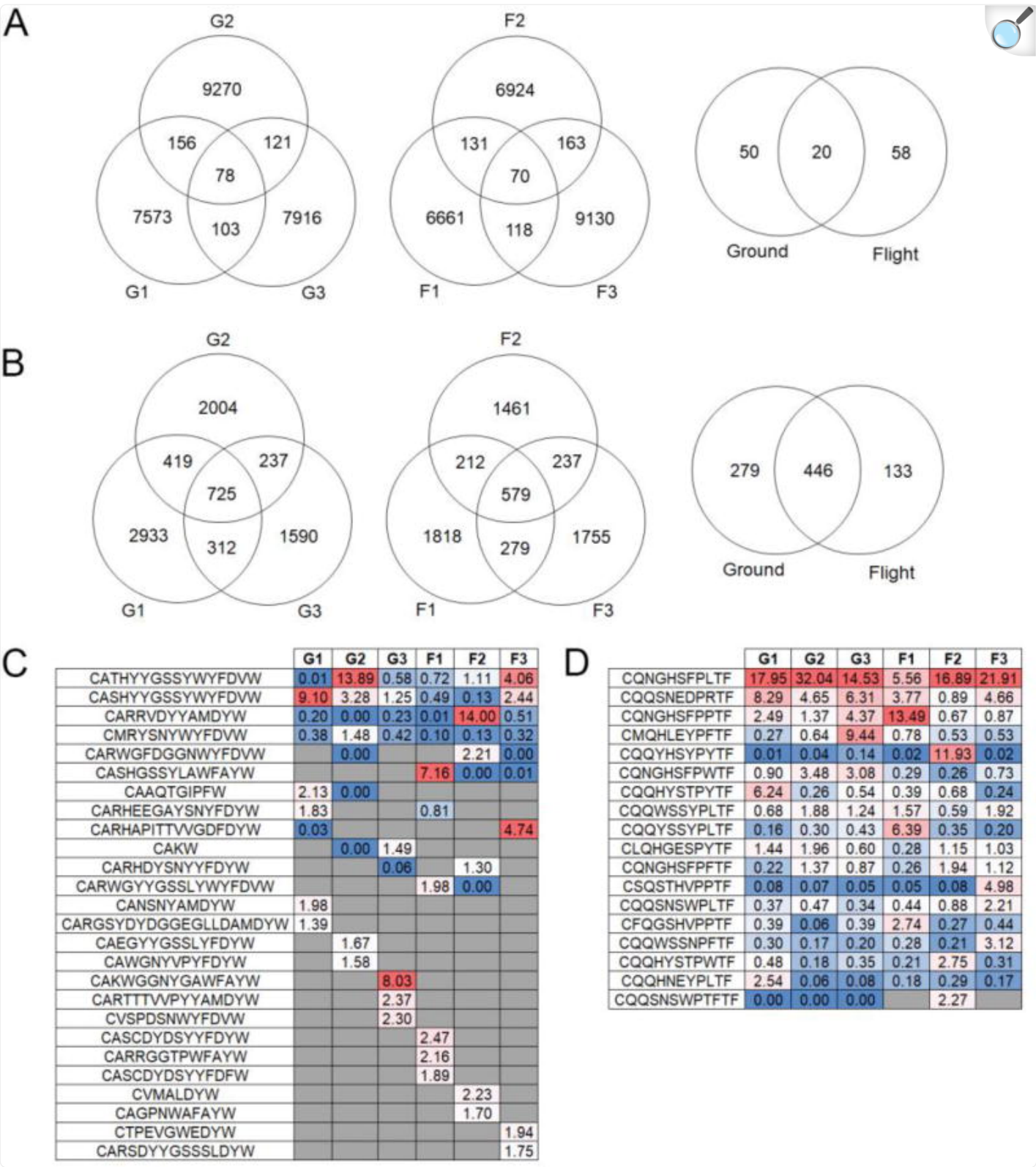
[Open in a new tab](#)

The mean-average CDR3 length of ground control (G) and flight (F) animals is displayed by isotype. Assessment by two-way ANOVA revealed no significant differences in CDR3 length by treatment group ($p=0.6225$), isotype ($p=0.4589$), or the interaction of the two variables

Kappa-chain CDR3 length was conserved at nine amino acids with 90.3 to 94.2 percent of all light chains having CDR3 rearrangements that were nine amino acids in length (Figure 5B). Only a small percentage of light chains had eight amino acids (2.8 to 6.9%), or ten amino acid long (0.9–3.9%) CDR3s. Ground mouse one (0.9%), was an exception and was enriched for 11 amino acid CDR3s (2.3%) compared to other animals (0.2–0.7%). CDR3 lengths over 18 amino acids were not displayed (20, 25, 27, 29, 32, 35, 36, 37, 39). CDR3 rearrangements of these lengths were often only detected in one animal and expression of these lengths did not exceed 0.01% of the repertoire. Additionally, these rearrangements may have been identified in error as many of these rearrangements contain intervening phenylalanine residues within the There was little overlap among IgH CDR3s regardless of treatment (Figure 6A, C). Of the top five CDR3s found in each animal, we identified 26 unique CDR3 AA rearrangements. Of those 26 CDR3s, four were found

in all six animals. Two additional rearrangements were identified in three animals. One of those rearrangements, CASHGSSYLAWFAYW, was found in only flight animals and not found in any ground animals. Six CDR3s were found in two animals, and the remainder were found in a single animal. The vast majority of CDR3 rearrangements detected were unique to each animal (6,661–9,270 rearrangements), though there was a small amount of overlap among animals (103–163 CDR3 rearrangements). For flight animals, 78 CDR3 rearrangements were found in all three animals and 70 were found in all three ground animals. Of the rearrangements found in all three animals per treatment group, only 20 rearrangements were detected in all six animals.

Figure 6. Top CDR3 Usage and Overlap of CDR3 Between Treatment Animals.



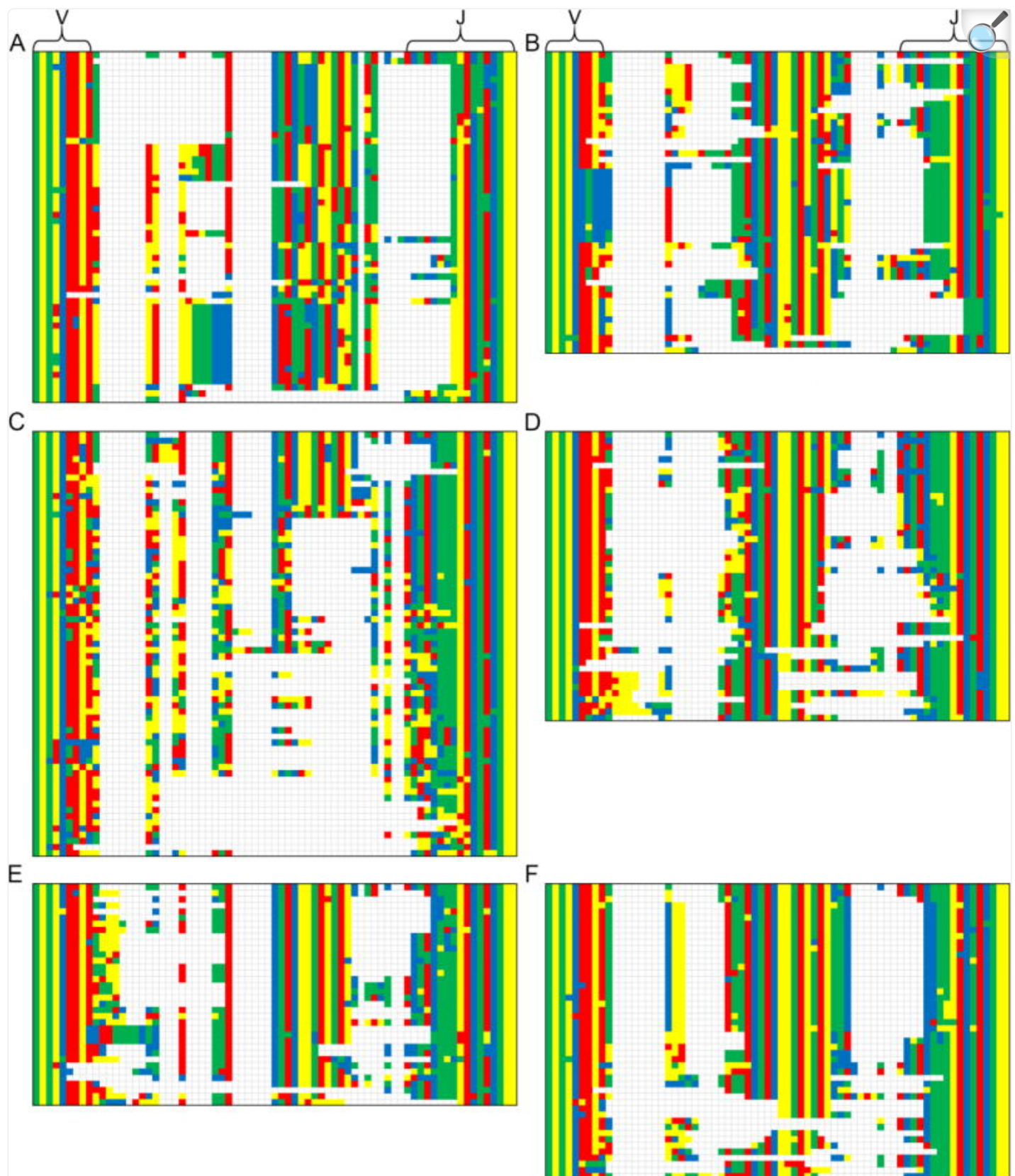
[Open in a new tab](#)

Venn diagrams show the overlap of unique CDR3 sequences among and between ground control (G1-G3) and flight treatment (F1-F3) groups in (A) IgH and (B) Igκ. CDR3 sequences were ranked within the top 5 most abundant rearrangements of any ground control or flight animals in (C) IgH and (D) Igκ. Dark red indicates higher percent of repertoire moving to blue, which represents lower percent of repertoire.

There was considerable overlap in the top five Igκ CDR3 rearrangements of each animal ([Figure 6B, D](#)). Seventeen total top CDR3 rearrangements were identified and all CDR3 rearrangements were identified in every animal. One CDR3 was the most abundant rearrangements in five animals (CQNGHSFPLTF), still ranking third in the remaining animal (F1). Ground control and flight animals shared three rearrangements that ranked within the top 20 CDR3 in all animals. Overall, between 1,590–2,933 unique CDR3 were detected in ground control animals, and between 1,461–1,818 unique CDR3 were detected in all flight animals ([Figure 6](#)). Of the 725 and 579 CDR3 shared in all three ground control and flight animals, respectively, 446 were shared between all six ground and flight animals.

A CDR3 rearrangement nucleotide sequence alignment of one of the top V-D-J-gene segment combinations demonstrates significant variability among mice such that any variability between ground and flight treatment groups cannot be determined with confidence ([Figure 7](#)). Additional data sets are needed in order to assess the effect of spaceflight on CDR3 formation.

Figure 7. Nucleotide Alignment of CDR3 from top V-D-J Combination.

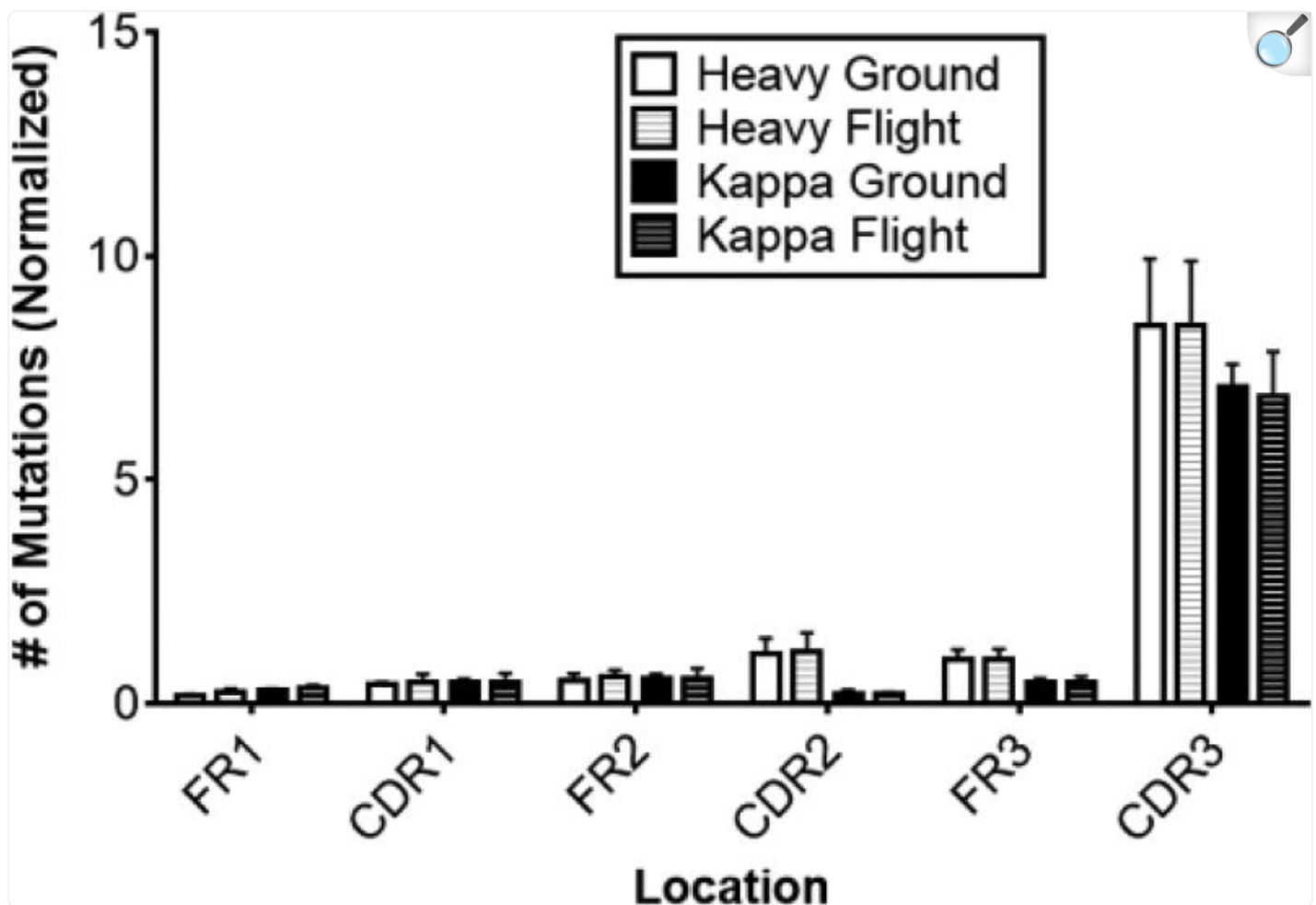


Nucleotide alignment of heavy-chain gene segment V1-26*01/D1-1*01/J1*03 across individuals in ground (G1 - A, G2 - C, G3 - E) and flight (F1 - B, F2 - D, F3 - F) treatment groups. Brackets in the germline region of the first individual in each treatment group delineate V- and J-gene regions. These bracketed regions remain the same across all individuals in the treatment group.

3.5 Mutations in Complementarity Determining and Framework Regions

We also examined mutation frequencies in CDR and framework (FW) regions for each animal because mutations can affect Ig specificity. Mutation frequencies were normalized by animal and Ig region (FW1-3, CDR1-3) by dividing the percent of total substitution mutations (total mutations/total productive reads) by respective region length ([Figure 8](#)). There were no significant differences between the mutation frequencies of ground control and flight animals for any of the Ig regions in both IgH (Student's *t*-test, $0.1916 < p < 0.9978$) and Igk (Student's *t*-test, $0.3175 < p < 0.9865$). When comparing the substitution mutation frequency across Ig regions, more substitution mutations occurred in CDR3 compared to other regions in IgH and Igk (ANOVA; all $p < 0.05$).

Figure 8. Substitution Mutations by Ig Region.



[Open in a new tab](#)

Total number of substitution mutations in FRs 1–3 and CDRs 1–3 were observed for both IgH and Igk chains. Abundance was first normalized by region length and then by total number of cleaned, productive reads in each respective data set and multiplied by 100 to attain percent abundance.

4 Discussion

Spaceflight and ground-based analog models induce phenotypic and functional changes in T- and B- lymphocyte populations. Spaceflight also affects bone marrow, the site of B-cell differentiation and development. Therefore, we wanted to know whether the stress and physiological changes associated with spaceflight would affect the normal development of the highly-diversified and highly-specific antigen receptors on B-lymphocytes. If so, the ability to

respond to pathogens might be affected. We characterized the antibody repertoire of C57BL/6Tac mice flown aboard the ISS and ground control animals using HTS and RNA-Seq.

HTS studies of antibody repertoires typically employ polymerase chain reaction amplification of Ig specific sequences from sorted B-cell populations. We assessed the B cell repertoire in whole spleen tissue because of the limitations of the primary science, a verification flight of mouse housing hardware. This precluded the sorting of cell populations. We previously showed that similar data could be generated using whole spleen tissue compared to whole spleen cell suspensions ([Rettig et al., 2017](#)). Although we do not account for B-cell subpopulations ([Yang et al., 2015](#), [Kaplinsky et al., 2014](#)), we do measure the total splenic Ig repertoire. Additionally, since we did not use specific amplification of Ig sequences the depth of sequencing was not as high as some have accomplished looking at Ig gene usage ([Yang et al., 2015](#), [Kaplinsky et al., 2014](#), [Menzel et al., 2014](#)). We have compared of amplified and unamplified data sets by our lab show reasonable correlations of the data, with more V-gene segments being detected in the unamplified data sets ([Rettig 2017](#), In Revision). Amplification with multiplex Ig specific primers may introduce amplification bias as primers may bind with varying efficiency to V-gene segments, although there have been recent advances in experimental approach to address amplification bias ([Wardemann, 2017](#)). We also found that the type of RNA-Seq analysis we are using in the assessment of younger C57Bl/6J mouse Ig gene usage, correlated well with that of studies using amplification ([Rettig et al., 2017](#)). Therefore, we feel we have a reasonable snapshot of B-cell receptors present in the spleens of 35-week-old female mice. In addition, the sample preparation allows additional data mining of valuable mouse samples.

In both humans and mice, early B-cell development occurs in the fetal liver prior to postnatal development in the bone marrow. We attempted to determine the Ig repertoire within the adult liver of the ground and flight animals in comparison to the splenic Ig repertoire. Unfortunately, few Ig sequences were recovered in liver samples suggesting few B cells are actually resident or circulating in the liver under normal, steady-state conditions. The liver kappa chain V-gene repertoire did correlate some with the usage in the spleen and probably reflects circulating B-cell Ig expression, but we did not confirm that. We focused our efforts on the spleen data.

While previous analyses by our lab used splenic mRNA pooled from four animals (Rettig et al., Submitted for Publication in PLOS ONE, ([Rettig et al., 2017](#))), the current study assessed individual mice and exhibited significantly more mouse-to-mouse variation than one might expect in inbred mice; even within treatment groups and compared to pooled mouse samples. Overall, V-gene segment usage correlated when analyzed using pairwise linear regression of animals within ground and flight treatment groups and there did not appear to be an impact of spaceflight on B-gene segment use. It is possible that differences in gene segment usage in ground and flight animals would be observed upon immunization. Studies on the effects of spaceflight in an immunized amphibian model showed altered VH-gene family and Ig class usage ([Boxio et al., 2005](#), [Bascove et al., 2009](#)).

We performed a number of analyses to determine if the Ig gene rearrangement process was affected by spaceflight. Averaged V-gene segment usage between the ground control and flight animals was moderately to highly correlated

(VH: $R^2=0.5922$, $p < 0.0001$; V κ : $R^2=0.831$, $p < 0.0001$). Many of the most abundant V-gene sequences were shared in flight and ground animals and there was no statistically significant difference in usage of individual top V-gene segments between ground control and flight animals (Student's *t*-test, $p=0.06478$ – 0.9609). Similarly, no differences in D-, JH- or J κ -gene segment usage and IgH constant region usage was seen between ground and flight animals.

We also examined whether spaceflight would affect the V/J-gene segment combinations that normally occur in specific pathogen-free mice. These too, were not different between ground control and flight animals for IgH and Ig κ . V/J-gene segment combinations were moderately to highly correlated (IgH: $R^2=0.3296$, Ig κ : $R^2=0.8795$, both $p < 0.0001$). An assessment of the impact of hypergravity on the similarly assembled T cell receptor repertoire of neonatal mice showed low correlation of individual Beta chain V- and J-gene segment recombination frequencies between control animals and animals subjected to centrifugation. 85% of gene V/J-gene segment combinations were not shared among the two treatment groups ([Ghislin et al., 2015](#)) and the differences could be attributed to changes in somatic recombination machinery under altered gravity conditions ([Schenten et al., 2013](#), [Ghislin et al., 2015](#)).

The combinatorial diversity of Ig was shown through the assessment of overall CDR3 sequence overlap among animals, as a large number of sequences were unique to only one animal. Little overlap was observed in the top 5 H-CDR3 rearrangements within all six ground and flight animals which totaled to 26 CDR3 rearrangements. Thirteen of these CDR3 rearrangements were only identified in one animal. More overlap was observed in the top 5 κ -CDR3 rearrangements within all six ground and flight animals which totaled 17 CDR3 rearrangements, which were identified in all animals.

The mice studied in this investigation were not challenged and were housed under specific-pathogen free conditions. Mutational frequency in Ig is normally associated with antigen stimulation ([Garcia et al., 1996](#)). Therefore, we did not expect that these mice were undergoing high amounts of somatic mutations. The majority of the mutations detected occurred in CDR3 in both ground and flight mice. It is possible that we will see differences in mutation frequency between ground control and flight animals after experimental immune challenge. The frequency of somatic hypermutations in *P. waltl* immunized in space was slightly lower than animals immunized on earth ([Bascove et al., 2011](#)). An experiment with antigen challenge of the Ig repertoire will be necessary to test this hypothesis.

The animals used in this experiment were older (35 weeks). The expression of genes necessary for Ig recombination do go down as mice age ([Cancro, 2009](#)). Therefore, it may be possible that we do not see differences between the treatment groups because the perturbations of spaceflight are not enough to disrupt the reduced B cell differentiations occurring in 35-week-old mice under normal steady-state conditions. Additionally, the half-life of B cells in secondary lymphoid organs is between four and seven weeks ([Fulcher and Basten, 1997](#)). Given the brief time that the mice were subjected to space flight (three weeks) it is likely that the exposure was not long enough to affect V/D/J recombination in the repertoire. Additional experiments, especially with young mice, will be needed to test this hypothesis.

Animals in this experiment were older and supplied from a different vendor (Taconic) than the 9–11-week-old C57BL/6J mice from Jackson Laboratories used in our previous experiments (([Rettig et al., 2017](#)), (Rettig et al., In Revision). To assess whether differences existed in the Ig repertoire, between the older C57BL/6Tac mice and the younger C57BL/6J mice, we compared gene segment usage between the two mouse cohorts. Because no differences in top V-gene segments, (D)J-gene segments, and constant region usage were detected between RR1 ground control and flight animals, all six animals were pooled and compared to the C57BL/6J cohort. We selected the 25 most abundant V-gene segments from both RR1 and C57BL/6J cohorts, resulting in 33 top IgHV and 34 top IgKV. We found that seven of 35 IgHV and eight of 32 IGKV were expressed at significantly different levels within the repertoire between the two cohorts (Student's *t*-test). These differences are largely driven by gene segments that are highly expressed in the RR1 cohort such as IGHV1-80, which represented $2.04 \pm 0.26\%$ of the repertoire in RR1 animals and $6.6 \pm 2.40\%$ of the repertoire in the C57BL/6J cohort (Student's *t*-test, $p=0.0032$). This is even more pronounced in IGKV5–39, which represented $21.41 \pm 7.50\%$ of the repertoire in RR1 animals and only $4.73 \pm 4.93\%$ of the repertoire in the C57BL/6J cohort (Student's *t*-test, $p=0.0109$).

We also performed a linear regression of top V-gene segment usage, which showed poor correlation between cohorts in both IgH ($R^2 = 0.1568$, $p=0.0226$) and IgK ($R^2 = 0.1681$, $p=0.0160$). D-gene segment usage was only significantly different IGHD1-1, which represented $39.7 \pm 5.23\%$ of the repertoire in RR1 animals and $26.49 \pm 0.94\%$ of the repertoire in the C57BL/6J cohort (Student's *t*-test, $p=0.0040$). We found that J-gene segment usage varied between the two cohorts in three out of five IGKJ and no differences in IGHV were detected (student's *t*-test). IgH constant region usage was significantly different for IgD (RR1: $0.63 \pm 0.22\%$, C57BL6/J: $4.60 \pm 0.69\%$; Student's *t*-test, $p=0.0074$) and IgG (RR1: $23.83 \pm 6.19\%$, C57BL6/J: $9.65 \pm 6.19\%$; Student's *t*-test, $p=0.0074$).

Although we cannot determine whether these differences are attributed to differences in vendor or differences in age, it is likely that repertoire differences are driven by a more mature Ig repertoire within the RR1 animals, as a higher percentage of IgH sequences demonstrate class switching. Both cohorts were unimmunized and maintained under specific pathogen-free conditions.

In conclusion, we have been able to successfully characterize immunoglobulin gene segment usage and junctional diversity within the antibody repertoire of unimmunized C57BL/6Tac mice flown aboard the ISS. Individual gene segment usage remained similar among animals within and among treatment groups, with the most abundant gene segments being conserved across all animals. Gene segment combinations and CDR3 sequences were highly varied, demonstrating the combinatorial diversity of the antibody repertoire, but that variation reflects the dynamics of individualized selection of Ig molecules and not any impact of spaceflight. A larger sample size would help solidify this conclusion, but these data provide preliminary suggestions that the recombinatorial processes that lead to the diverse Ig repertoires in mice are not affected by a short trip to and stay on the ISS. These data do not preclude that differences in the Ig repertoires of ground and flight animals will not be seen during active immunization or in younger, possibly more recombinatorily active mice. Current studies in our lab aim to characterize antibody repertoire dynamics upon antigen

challenge using a murine anti-orthostatic suspension model and during a future space flight.

Supplementary Material

1

[NIHMS928411-supplement-1.xml](#) (410B, xml)

2

[NIHMS928411-supplement-2.pdf](#) (954.1KB, pdf)

3

[NIHMS928411-supplement-3.pdf](#) (229KB, pdf)

4

[NIHMS928411-supplement-4.tif](#) (3.4MB, tif)

5

[NIHMS928411-supplement-5.pdf](#) (82.9KB, pdf)

Footnotes

Publisher's Disclaimer: This is a PDF file of an unedited manuscript that has been accepted for publication. As a service to our customers we are providing this early version of the manuscript. The manuscript will undergo copyediting, typesetting, and review of the resulting proof before it is published in its final citable form. Please note that during the production process errors may be discovered which could affect the content, and all legal disclaimers that apply to the journal pertain.

References

1. Ademokun A, Wu YC, Martin V, Mitra R, Sack U, Baxendale H, Kipling D, Dunn-Walters DK. Vaccination-Induced Changes In Human B-Cell Repertoire And Pneumococcal Igm And Iga Antibody At Different Ages. *Aging Cell*. 2011;10:922–30. doi: 10.1111/j.1474-9726.2011.00732.x. [[DOI](#)] [[PMC free article](#)] [[PubMed](#)] [[Google Scholar](#)]
2. Alamyar E, Duroux P, Lefranc MP, Giudicelli V. Igmgt((R)) Tools For The Nucleotide Analysis Of Immunoglobulin (Ig) And T Cell Receptor (Tr) V-(D)-J Repertoires, Polymorphisms, And Ig Mutations: Igmgt/V-Quest And Igmgt/Highv-Quest For Ngs. *Methods Mol Biol*. 2012;882:569–604. doi: 10.1007/978-1-61779-842-9_32. [[DOI](#)] [[PubMed](#)] [[Google Scholar](#)]
3. Allebban Z, Ichiki AT, Gibson LA, Jones JB, Congdon CC, Lange RD. Effects Of Spaceflight On The Number Of Rat Peripheral Blood Leukocytes And Lymphocyte Subsets. *J Leukoc Biol*. 1994;55:209–13. doi: 10.1002/jlb.55.2.209. [[DOI](#)] [[PubMed](#)] [[Google Scholar](#)]
4. Alt FW, Yancopoulos GD, Blackwell TK, Wood C, Thomas E, Boss M, Coffman R, Rosenberg N, Tonegawa S, Baltimore D. Ordered Rearrangement Of Immunoglobulin Heavy Chain Variable Region Segments. *Embo J*. 1984;3:1209–19. doi: 10.1002/j.1460-2075.1984.tb01955.x. [[DOI](#)] [[PMC free article](#)] [[PubMed](#)] [[Google Scholar](#)]
5. Armstrong JW, Nelson KA, Simske SJ, Luttges MW, Iandolo JJ, Chapes SK. Skeletal Unloading Causes Organ-Specific Changes In Immune Cell Responses. *J Appl Physiol* (1985) 1993;75:2734–9. doi: 10.1152/jappl.1993.75.6.2734. [[DOI](#)] [[PubMed](#)] [[Google Scholar](#)]
6. Baqai FP, Gridley DS, Slater JM, Luo-Owen X, Stodieck LS, Ferguson V, Chapes SK, Pecaut MJ. Effects Of Spaceflight On Innate Immune Function And Antioxidant Gene Expression. *J Appl Physiol* (1985) 2009;106:1935–42. doi: 10.1152/japplphysiol.91361.2008. [[DOI](#)] [[PMC free article](#)] [[PubMed](#)] [[Google Scholar](#)]
7. Bascove M, Gueguinou N, Schaerlinger B, Gauquelin-Koch G, Fripiat JP. Decrease In Antibody Somatic

Hypermutation Frequency Under Extreme, Extended Spaceflight Conditions. *Faseb J.* 2011;25:2947–55. doi: 10.1096/fj.11-185215. [[DOI](#)] [[PubMed](#)] [[Google Scholar](#)]

8. Bascove M, Huin-Schohn C, Gueguinou N, Tschirhart E, Fripiat JP. Spaceflight-Associated Changes In Immunoglobulin Vh Gene Expression In The Amphibian *Pleurodeles Waltl*. *Faseb J.* 2009;23:1607–15. doi: 10.1096/fj.08-121327. [[DOI](#)] [[PubMed](#)] [[Google Scholar](#)]

9. Bashford-Rogers RJ, Nicolaou KA, Bartram J, Goulden NJ, Loizou L, Koumas L, Chi J, Hubank M, Kellam P, Costeas PA, Vassiliou GS. Eye On The B-All: B-Cell Receptor Repertoires Reveal Persistence Of Numerous B-Lymphoblastic Leukemia Subclones From Diagnosis To Relapse. *Leukemia.* 2016;30:2312–2321. doi: 10.1038/leu.2016.142. [[DOI](#)] [[PMC free article](#)] [[PubMed](#)] [[Google Scholar](#)]

10. Berry CA. Summary Of Medical Experience In The Apollo 7 Through 11 Manned Spaceflights. *Aerosp Med.* 1970;41:500–19. [[PubMed](#)] [[Google Scholar](#)]

11. Boxio R, Dournon C, Fripiat JP. Effects Of A Long-Term Spaceflight On Immunoglobulin Heavy Chains Of The Urodele Amphibian *Pleurodeles Waltl*. *J Appl Physiol (1985)* 2005;98:905–10. doi: 10.1152/japplphysiol.00957.2004. [[DOI](#)] [[PubMed](#)] [[Google Scholar](#)]

12. Cancro MPHY, Scholz JL, Riley RL, Frasca D, Dunn-Walters DK, Blomberg BB. B Cells And Aging: Molecules And Mechanisms. *Trends In Immunology.* 2009;30:313–318. doi: 10.1016/j.it.2009.04.005. [[DOI](#)] [[PMC free article](#)] [[PubMed](#)] [[Google Scholar](#)]

13. Chang TT, Walther I, Li CF, Boonyaratanakornkit J, Galleri G, Meloni MA, Pippia P, Cogoli A, Hughes-Fulford M. The Rel/Nf-Kappab Pathway And Transcription Of Immediate Early Genes In T Cell Activation Are Inhibited By Microgravity. *J Leukoc Biol.* 2012;92:1133–45. doi: 10.1189/jlb.0312157. [[DOI](#)] [[PMC free article](#)] [[PubMed](#)] [[Google Scholar](#)]

14. Chapes SK, Mastro AM, Sonnenfeld G, Berry WD. Antiorthostatic Suspension As A Model For The Effects Of Spaceflight On The Immune System. *J Leukoc Biol.* 1993;54:227–35. doi: 10.1002/jlb.54.3.227. [[DOI](#)] [[PubMed](#)] [[Google Scholar](#)]

15. Chapes SK, Simske SJ, Forsman AD, Bateman TA, Zimmerman RJ. Effects Of Space Flight And Igf-1 On Immune Function. *Adv Space Res.* 1999A;23:1955–64. doi: 10.1016/s0273-1177(99)00456-1. [[DOI](#)] [[PubMed](#)] [[Google Scholar](#)]

16. Chapes SK, Simske SJ, Sonnenfeld G, Miller ES, Zimmerman RJ. Effects Of Spaceflight And Peg-Il-2 On Rat Physiological And Immunological Responses. *J Appl Physiol (1985)* 1999B;86:2065–76. doi: 10.1152/jappl.1999.86.6.2065. [[DOI](#)] [[PubMed](#)] [[Google Scholar](#)]

17. Cogoli-Greuter M. Effect Of Gravity Changes On The Cytoskeleton In Human Lymphocytes.

Gravitational And Space Biology Bulletin. 2004;17:27–38. [[Google Scholar](#)]

18. Cogoli A, Tschopp A, Fuchs-Bislin P. Cell Sensitivity To Gravity. *Science*. 1984;225:228–30. doi: 10.1126/science.6729481. [[DOI](#)] [[PubMed](#)] [[Google Scholar](#)]

19. Congdon CC, Allebban Z, Gibson LA, Kaplansky A, Strickland KM, Jago TL, Johnson DL, Lange RD, Ichiki AT. Lymphatic Tissue Changes In Rats Flown On Spacelab Life Sciences-2. *J Appl Physiol* (1985) 1996;81:172–7. doi: 10.1152/jappl.1996.81.1.172. [[DOI](#)] [[PubMed](#)] [[Google Scholar](#)]

20. Cooper D, Pride MW, Brown EL, Risin D, Pellis NR. Suppression Of Antigen-Specific Lymphocyte Activation In Modeled Microgravity. *In Vitro Cell Dev Biol Anim*. 2001;37:63–5. doi: 10.1290/1071-2690(2001)037<0063:SOASLA>2.0.CO;2. [[DOI](#)] [[PubMed](#)] [[Google Scholar](#)]

21. Crucian B, Simpson RJ, Mehta S, Stowe R, Chouker A, Hwang SA, Actor JK, Salam AP, Pierson D, Sams C. Terrestrial Stress Analogs For Spaceflight Associated Immune System Dysregulation. *Brain Behav Immun*. 2014A;39:23–32. doi: 10.1016/j.bbi.2014.01.011. [[DOI](#)] [[PubMed](#)] [[Google Scholar](#)]

22. Crucian B, Stowe R, Mehta S, Uchakin P, Quiriarte H, Pierson D, Sams C. Immune System Dysregulation Occurs During Short Duration Spaceflight On Board The Space Shuttle. *J Clin Immunol*. 2013;33:456–65. doi: 10.1007/s10875-012-9824-7. [[DOI](#)] [[PubMed](#)] [[Google Scholar](#)]

23. Crucian BE, Zwart SR, Mehta S, Uchakin P, Quiriarte HD, Pierson D, Sams CF, Smith SM. Plasma Cytokine Concentrations Indicate That In Vivo Hormonal Regulation Of Immunity Is Altered During Long-Duration Spaceflight. *J Interferon Cytokine Res*. 2014B;34:778–86. doi: 10.1089/jir.2013.0129. [[DOI](#)] [[PMC free article](#)] [[PubMed](#)] [[Google Scholar](#)]

24. Durnova GN, Kaplansky AS, Portugalov VV. Effect Of A 22-Day Space Flight On The Lymphoid Organs Of Rats. *Aviat Space Environ Med*. 1976;47:588–91. [[PubMed](#)] [[Google Scholar](#)]

25. Early P, Huang H, Davis M, Calame K, Hood L. An Immunoglobulin Heavy Chain Variable Region Gene Is Generated From Three Segments Of Dna: Vh, D And Jh. *Cell*. 1980;19:981–92. doi: 10.1016/0092-8674(80)90089-6. [[DOI](#)] [[PubMed](#)] [[Google Scholar](#)]

26. Fitzgerald W, Chen S, Walz C, Zimmerberg J, Margolis L, Grivel JC. Immune Suppression Of Human Lymphoid Tissues And Cells In Rotating Suspension Culture And Onboard The International Space Station. *In Vitro Cell Dev Biol Anim*. 2009;45:622–32. doi: 10.1007/s11626-009-9225-2. [[DOI](#)] [[PMC free article](#)] [[PubMed](#)] [[Google Scholar](#)]

27. Fulcher DA, Basten A. B Cell Life Span: A Review. *Immunol Cell Biol*. 1997;75:446–55. doi: 10.1038/icb.1997.69. [[DOI](#)] [[PubMed](#)] [[Google Scholar](#)]

28. Gaignier F, Schenten V, De Carvalho Bittencourt M, Gauquelin-Koch G, Fripiat JP, Legrand-Frossi C.

Three Weeks Of Murine Hindlimb Unloading Induces Shifts From B To T And From Th To Tc Splenic Lymphocytes In Absence Of Stress And Differentially Reduces Cell-Specific Mitogenic Responses. *Plos One*. 2014;9:E92664. doi: 10.1371/journal.pone.0092664. [[DOI](#)] [[PMC free article](#)] [[PubMed](#)] [[Google Scholar](#)]

29. Garcia KC, Scott CA, Brunmark A, Carbone FR, Peterson PA, Wilson IA, Teyton L. Cd8 Enhances Formation Of Stable T-Cell Receptor/Mhc Class I Molecule Complexes. *Nature*. 1996;384:577–581. doi: 10.1038/384577a0. [[DOI](#)] [[PubMed](#)] [[Google Scholar](#)]

30. Georgiou G, Ippolito GC, Beausang J, Busse CE, Wardemann H, Quake SR. The Promise And Challenge Of High-Throughput Sequencing Of The Antibody Repertoire. *Nat Biotechnol*. 2014;32:158–68. doi: 10.1038/nbt.2782. [[DOI](#)] [[PMC free article](#)] [[PubMed](#)] [[Google Scholar](#)]

31. Ghislin S, Ouzren-Zarhloul N, Kaminski S, Fripiat JP. Hypergravity Exposure During Gestation Modifies The Tcrbeta Repertoire Of Newborn Mice. *Sci Rep*. 2015;5:9318. doi: 10.1038/srep09318. [[DOI](#)] [[PMC free article](#)] [[PubMed](#)] [[Google Scholar](#)]

32. Gilfillan S, Dierich A, Lemeur M, Benoist C, Mathis D. Mice Lacking Tdt: Mature Animals With An Immature Lymphocyte Repertoire. *Science*. 1993;261:1175–8. doi: 10.1126/science.8356452. [[DOI](#)] [[PubMed](#)] [[Google Scholar](#)]

33. Globus RK, Morey-Holton E. Hindlimb Unloading: Rodent Analog For Microgravity. *J Appl Physiol* (1985) 2016;120:1196–206. doi: 10.1152/jappphysiol.00997.2015. [[DOI](#)] [[PubMed](#)] [[Google Scholar](#)]

34. Greiff V, Bhat P, Cook SC, Menzel U, Kang W, Reddy ST. A Bioinformatic Framework For Immune Repertoire Diversity Profiling Enables Detection Of Immunological Status. *Genome Med*. 2015;7:49. doi: 10.1186/s13073-015-0169-8. [[DOI](#)] [[PMC free article](#)] [[PubMed](#)] [[Google Scholar](#)]

35. Gridley DS, Mao XW, Stodieck LS, Ferguson VL, Bateman TA, Moldovan M, Cunningham CE, Jones TA, Slater JM, Pecaut MJ. Changes In Mouse Thymus And Spleen After Return From The Sts-135 Mission In Space. *Plos One*. 2013;8:E75097. doi: 10.1371/journal.pone.0075097. [[DOI](#)] [[PMC free article](#)] [[PubMed](#)] [[Google Scholar](#)]

36. Gridley DS, Slater JM, Luo-Owen X, Rizvi A, Chapes SK, Stodieck LS, Ferguson VL, Pecaut MJ. Spaceflight Effects On T Lymphocyte Distribution, Function And Gene Expression. *J Appl Physiol* (1985) 2009;106:194–202. doi: 10.1152/jappphysiol.91126.2008. [[DOI](#)] [[PMC free article](#)] [[PubMed](#)] [[Google Scholar](#)]

37. Grigoriev AI, Bugrov SA, Bogomolov VV, Egorov AD, Polyakov VV, Tarasov IK, Shulzhenko EB. Main Medical Results Of Extended Flights On Space Station Mir In 1986–1990. *Acta Astronaut*. 1993;29:581–5. doi: 10.1016/0094-5765(93)90073-6. [[DOI](#)] [[PubMed](#)] [[Google Scholar](#)]

38. Grove DS, Pishak SA, Mastro AM. The Effect Of A 10-Day Space Flight On The Function, Phenotype, And Adhesion Molecule Expression Of Splenocytes And Lymph Node Lymphocytes. *Exp Cell Res*. 1995;219:102–9. doi: 10.1006/excr.1995.1210. [[DOI](#)] [[PubMed](#)] [[Google Scholar](#)]
39. Hozumi N, Tonegawa S. Evidence For Somatic Rearrangement Of Immunoglobulin Genes Coding For Variable And Constant Regions. *Proc Natl Acad Sci U S A*. 1976;73:3628–32. doi: 10.1073/pnas.73.10.3628. [[DOI](#)] [[PMC free article](#)] [[PubMed](#)] [[Google Scholar](#)]
40. Huin-Schohn C, Gueguinou N, Schenten V, Bascove M, Koch GG, Baatout S, Tschirhart E, Fripiat JP. Gravity Changes During Animal Development Affect Igm Heavy-Chain Transcription And Probably Lymphopoiesis. *Faseb J*. 2013;27:333–41. doi: 10.1096/fj.12-217547. [[DOI](#)] [[PubMed](#)] [[Google Scholar](#)]
41. Hwang SA, Crucian B, Sams C, Actor JK. Post-Spaceflight (Sts-135) Mouse Splenocytes Demonstrate Altered Activation Properties And Surface Molecule Expression. *Plos One*. 2015;10:E0124380. doi: 10.1371/journal.pone.0124380. [[DOI](#)] [[PMC free article](#)] [[PubMed](#)] [[Google Scholar](#)]
42. Ichiki AT, Gibson LA, Jago TL, Strickland KM, Johnson DL, Lange RD, Allebban Z. Effects Of Spaceflight On Rat Peripheral Blood Leukocytes And Bone Marrow Progenitor Cells. *J Leukoc Biol*. 1996;60:37–43. doi: 10.1002/jlb.60.1.37. [[DOI](#)] [[PubMed](#)] [[Google Scholar](#)]
43. Jiang Y, Nie K, Redmond D, Melnick AM, Tam W, Elemento O. Vdj-Seq: Deep Sequencing Analysis Of Rearranged Immunoglobulin Heavy Chain Gene To Reveal Clonal Evolution Patterns Of B Cell Lymphoma. *J Vis Exp*. 2015:E53215. doi: 10.3791/53215. [[DOI](#)] [[PMC free article](#)] [[PubMed](#)] [[Google Scholar](#)]
44. Kabat EA, Wu TT, Bilofsky H. Evidence Supporting Somatic Assembly Of The Dna Segments (Minigenes), Coding For The Framework, And Complementarity-Determining Segments Of Immunoglobulin Variable Regions. *J Exp Med*. 1979;149:1299–313. doi: 10.1084/jem.149.6.1299. [[DOI](#)] [[PMC free article](#)] [[PubMed](#)] [[Google Scholar](#)]
45. Kaplinsky J, Li A, Sun A, Coffre M, Koralov SB, Arnaout R. Antibody Repertoire Deep Sequencing Reveals Antigen-Independent Selection In Maturing B Cells. *Proc Natl Acad Sci U S A*. 2014;111:E2622–9. doi: 10.1073/pnas.1403278111. [[DOI](#)] [[PMC free article](#)] [[PubMed](#)] [[Google Scholar](#)]
46. Katoh K, Misawa K, Kuma K, Miyata T. Mafft: A Novel Method For Rapid Multiple Sequence Alignment Based On Fast Fourier Transform. *Nucleic Acids Res*. 2002;30:3059–66. doi: 10.1093/nar/gkf436. [[DOI](#)] [[PMC free article](#)] [[PubMed](#)] [[Google Scholar](#)]
47. Khurana S, Fuentes S, Coyle EM, Ravichandran S, Davey RT, Jr, Beigel JH. Human Antibody Repertoire After Vsv-Ebola Vaccination Identifies Novel Targets And Virus-Neutralizing Igm Antibodies. *Nat Med*. 2016;22:1439–1447. doi: 10.1038/nm.4201. [[DOI](#)] [[PubMed](#)] [[Google Scholar](#)]

48. Komori T, Okada A, Stewart V, Alt FW. Lack Of N Regions In Antigen Receptor Variable Region Genes Of Tdt-Deficient Lymphocytes. *Science*. 1993;261:1171–5. doi: 10.1126/science.8356451. [[DOI](#)] [[PubMed](#)] [[Google Scholar](#)]
49. Krzywinski M, Schein J, Birol I, Connors J, Gascoyne R, Horsman D, Jones SJ, Marra MA. Circos: An Information Aesthetic For Comparative Genomics. *Genome Res*. 2009;19:1639–45. doi: 10.1101/gr.092759.109. [[DOI](#)] [[PMC free article](#)] [[PubMed](#)] [[Google Scholar](#)]
50. Lee J, Boutz DR, Chromikova V, Joyce MG, Vollmers C, Leung K, Horton AP, Dekosky BJ, Lee CH, Lavinder JJ, Murrin EM, Chrysostomou C, Hoi KH, Tsybovsky Y, Thomas PV, Druz A, Zhang B, Zhang Y, Wang L, Kong WP, Park D, Popova LI, Dekker CL, Davis MM, Carter CE, Ross TM, Ellington AD, Wilson PC, Marcotte EM, Mascola JR, Ippolito GC, Krammer F, Quake SR, Kwong PD, Georgiou G. Molecular-Level Analysis Of The Serum Antibody Repertoire In Young Adults Before And After Seasonal Influenza Vaccination. *Nat Med*. 2016;22:1456–1464. doi: 10.1038/nm.4224. [[DOI](#)] [[PMC free article](#)] [[PubMed](#)] [[Google Scholar](#)]
51. Lescale C, Schenten V, Djeghloul D, Bennabi M, Gaignier F, Vandamme K, Strazielle C, Kuzniak I, Petite H, Dosquet C, Fripiat JP, Goodhardt M. Hind Limb Unloading, A Model Of Spaceflight Conditions, Leads To Decreased B Lymphopoiesis Similar To Aging. *Faseb J*. 2015;29:455–63. doi: 10.1096/fj.14-259770. [[DOI](#)] [[PubMed](#)] [[Google Scholar](#)]
52. Lesnyak A, Sonnenfeld G, Avery L, Konstantinova I, Rykova M, Meshkov D, Orlova T. Effect Of Sls-2 Spaceflight On Immunologic Parameters Of Rats. *J Appl Physiol* (1985) 1996;81:178–82. doi: 10.1152/jappl.1996.81.1.178. [[DOI](#)] [[PubMed](#)] [[Google Scholar](#)]
53. Lesnyak AT, Sonnenfeld G, Rykova MP, Meshkov DO, Mastro A, Konstantinova I. Immune Changes In Test Animals During Spaceflight. *J Leukoc Biol*. 1993;54:214–26. doi: 10.1002/jlb.54.3.214. [[DOI](#)] [[PubMed](#)] [[Google Scholar](#)]
54. Loder F, Mutschler B, Ray RJ, Paige CJ, Sideras P, Torres R, Lamers MC, Carsetti R. B Cell Development In The Spleen Takes Place In Discrete Steps And Is Determined By The Quality Of B Cell Receptor-Derived Signals. *J Exp Med*. 1999;190:75–89. doi: 10.1084/jem.190.1.75. [[DOI](#)] [[PMC free article](#)] [[PubMed](#)] [[Google Scholar](#)]
55. Logan AC, Gao H, Wang C, Sahaf B, Jones CD, Marshall EL, Buno I, Armstrong R, Fire AZ, Weinberg KI, Mindrinos M, Zehnder JL, Boyd SD, Xiao W, Davis RW, Miklos DB. High-Throughput Vdj Sequencing For Quantification Of Minimal Residual Disease In Chronic Lymphocytic Leukemia And Immune Reconstitution Assessment. *Proc Natl Acad Sci U S A*. 2011;108:21194–9. doi: 10.1073/pnas.1118357109. [[DOI](#)] [[PMC free article](#)] [[PubMed](#)] [[Google Scholar](#)]

56. Martinez EM, Yoshida MC, Candelario TL, Hughes-Fulford M. Spaceflight And Simulated Microgravity Cause A Significant Reduction Of Key Gene Expression In Early T-Cell Activation. *Am J Physiol Regul Integr Comp Physiol*. 2015;308:R480–8. doi: 10.1152/ajpregu.00449.2014. [[DOI](#)] [[PMC free article](#)] [[PubMed](#)] [[Google Scholar](#)]
57. Menzel U, Greiff V, Khan TA, Haessler U, Hellmann I, Friedensohn S, Cook SC, Pogson M, Reddy ST. Comprehensive Evaluation And Optimization Of Amplicon Library Preparation Methods For High-Throughput Antibody Sequencing. *Plos One*. 2014;9:E96727. doi: 10.1371/journal.pone.0096727. [[DOI](#)] [[PMC free article](#)] [[PubMed](#)] [[Google Scholar](#)]
58. Montesinos-Rongen M, Purschke F, Kuppers R, Deckert M. Immunoglobulin Repertoire Of Primary Lymphomas Of The Central Nervous System. *J Neuropathol Exp Neurol*. 2014;73:1116–25. doi: 10.1097/NEN.0000000000000133. [[DOI](#)] [[PubMed](#)] [[Google Scholar](#)]
59. Nash PV, Konstantinova IV, Fuchs BB, Rakhmilevich AL, Lesnyak AT, Mastro AM. Effect Of Spaceflight On Lymphocyte Proliferation And Interleukin-2 Production. *J Appl Physiol* (1985) 1992;73:186S–190S. doi: 10.1152/jappl.1992.73.2.S186. [[DOI](#)] [[PubMed](#)] [[Google Scholar](#)]
60. Nash PV, Mastro AM. Variable Lymphocyte Responses In Rats After Space Flight. *Exp Cell Res*. 1992;202:125–31. doi: 10.1016/0014-4827(92)90411-z. [[DOI](#)] [[PubMed](#)] [[Google Scholar](#)]
61. Nickerson CA, Ott CM, Wilson JW, Ramamurthy R, Leblanc CL, Honer Zu Bentrup K, Hammond T, Pierson DL. Low-Shear Modeled Microgravity: A Global Environmental Regulatory Signal Affecting Bacterial Gene Expression, Physiology, And Pathogenesis. *J Microbiol Methods*. 2003;54:1–11. doi: 10.1016/s0167-7012(03)00018-6. [[DOI](#)] [[PubMed](#)] [[Google Scholar](#)]
62. Ortega MT, Pecaut MJ, Gridley DS, Stodieck LS, Ferguson V, Chapes SK. Shifts In Bone Marrow Cell Phenotypes Caused By Spaceflight. *J Appl Physiol* (1985) 2009;106:548–55. doi: 10.1152/japplphysiol.91138.2008. [[DOI](#)] [[PMC free article](#)] [[PubMed](#)] [[Google Scholar](#)]
63. Parameswaran P, Liu Y, Roskin KM, Jackson KK, Dixit VP, Lee JY, Artiles KL, Zompi S, Vargas MJ, Simen BB, Hanczaruk B, McGowan KR, Tariq MA, Pourmand N, Koller D, Balmaseda A, Boyd SD, Harris E, Fire AZ. Convergent Antibody Signatures In Human Dengue. *Cell Host Microbe*. 2013;13:691–700. doi: 10.1016/j.chom.2013.05.008. [[DOI](#)] [[PMC free article](#)] [[PubMed](#)] [[Google Scholar](#)]
64. Pecaut MJ, Nelson GA, Peters LL, Kostenuik PJ, Bateman TA, Morony S, Stodieck LS, Lacey DL, Simske SJ, Gridley DS. Genetic Models In Applied Physiology: Selected Contribution: Effects Of Spaceflight On Immunity In The C57Bl/6 Mouse. I. Immune Population Distributions. *J Appl Physiol* (1985) 2003;94:2085–94. doi: 10.1152/japplphysiol.01052.2002. [[DOI](#)] [[PubMed](#)] [[Google Scholar](#)]
65. Pecaut MJ, Simske SJ, Fleshner M. Spaceflight Induces Changes In Splenocyte Subpopulations:

Effectiveness Of Ground-Based Models. *Am J Physiol Regul Integr Comp Physiol*. 2000;279:R2072–8. doi: 10.1152/ajpregu.2000.279.6.R2072. [[DOI](#)] [[PubMed](#)] [[Google Scholar](#)]

66. Rettig TA, Ward C, Pecaut MJ, Chapes SK. Validation Of Methods To Assess The Immunoglobulin Gene Repertoire In Tissues Obtained From Mice On The International Space Station. *Gravitational And Space Research*. 2017;5:2–23. [[PMC free article](#)] [[PubMed](#)] [[Google Scholar](#)]

67. Rykova MP, Antropova EN, Larina IM, Morukov BV. Humoral And Cellular Immunity In Cosmonauts After The Iss Missions. *Acta Astronautica*. 2008;63:697–705. [[Google Scholar](#)]

68. Sakano H, Huppi K, Heinrich G, Tonegawa S. Sequences At The Somatic Recombination Sites Of Immunoglobulin Light-Chain Genes. *Nature*. 1979;280:288–94. doi: 10.1038/280288a0. [[DOI](#)] [[PubMed](#)] [[Google Scholar](#)]

69. Sanzari JK, Romero-Weaver AL, James G, Kringsfeld G, Lin L, Diffenderfer ES, Kennedy AR. Leukocyte Activity Is Altered In A Ground Based Murine Model Of Microgravity And Proton Radiation Exposure. *Plos One*. 2013;8:E71757. doi: 10.1371/journal.pone.0071757. [[DOI](#)] [[PMC free article](#)] [[PubMed](#)] [[Google Scholar](#)]

70. Schenten V, Gueguinou N, Baatout S, Fripiat JP. Modulation Of Pleurodeles Waltl Dna Polymerase Mu Expression By Extreme Conditions Encountered During Spaceflight. *Plos One*. 2013;8:E69647. doi: 10.1371/journal.pone.0069647. [[DOI](#)] [[PMC free article](#)] [[PubMed](#)] [[Google Scholar](#)]

71. Sonnenfeld G. Experimentation With Animal Models In Space. Introduction. *Adv Space Biol Med*. 2005;10:1–5. doi: 10.1016/s1569-2574(05)10001-x. [[DOI](#)] [[PubMed](#)] [[Google Scholar](#)]

72. Sonnenfeld G, Foster M, Morton D, Bailliard F, Fowler NA, Hakenewerth AM, Bates R, Miller ES, Jr Spaceflight And Development Of Immune Responses. *J Appl Physiol* (1985) 1998;85:1429–33. doi: 10.1152/jappl.1998.85.4.1429. [[DOI](#)] [[PubMed](#)] [[Google Scholar](#)]

73. Sonnenfeld G, Mandel AD, Konstantinova IV, Berry WD, Taylor GR, Lesnyak AT, Fuchs BB, Rakhmilevich AL. Spaceflight Alters Immune Cell Function And Distribution. *J Appl Physiol* (1985) 1992;73:191S–195S. doi: 10.1152/jappl.1992.73.2.S191. [[DOI](#)] [[PubMed](#)] [[Google Scholar](#)]

74. Sonnenfeld G, Mandel AD, Konstantinova IV, Taylor GR, Berry WD, Wellhausen SR, Lesnyak AT, Fuchs BB. Effects Of Spaceflight On Levels And Activity Of Immune Cells. *Aviat Space Environ Med*. 1990;61:648–53. [[PubMed](#)] [[Google Scholar](#)]

75. Stein TP, Schluter MD. Excretion Of Il-6 By Astronauts During Spaceflight. *Am J Physiol*. 1994;266:E448–52. doi: 10.1152/ajpendo.1994.266.3.E448. [[DOI](#)] [[PubMed](#)] [[Google Scholar](#)]

76. Stowe RP, Sams CF, Mehta SK, Kaur I, Jones ML, Feedback DL, Pierson DL. Leukocyte Subsets And

Neutrophil Function After Short-Term Spaceflight. *J Leukoc Biol.* 1999;65:179–86. doi: 10.1002/jlb.65.2.179.

[[DOI](#)] [[PubMed](#)] [[Google Scholar](#)]

77. Tan YC, Kongpachith S, Blum LK, Ju CH, Lahey LJ, Lu DR, Cai X, Wagner CA, Lindstrom TM, Sokolove J, Robinson WH. Barcode-Enabled Sequencing Of Plasmablast Antibody Repertoires In Rheumatoid Arthritis. *Arthritis Rheumatol.* 2014;66:2706–15. doi: 10.1002/art.38754. [[DOI](#)] [[PMC free article](#)] [[PubMed](#)] [[Google Scholar](#)]

78. Tan YG, Wang YQ, Zhang M, Han YX, Huang CY, Zhang HP, Li ZM, Wu XL, Wang XF, Dong Y, Zhu HM, Zhu SD, Li HM, Li N, Yan HP, Gao ZH. Clonal Characteristics Of Circulating B Lymphocyte Repertoire In Primary Biliary Cholangitis. *J Immunol.* 2016;197:1609–20. doi: 10.4049/jimmunol.1600096. [[DOI](#)] [[PubMed](#)] [[Google Scholar](#)]

79. Tauber S, Hauschild S, Paulsen K, Gutewort A, Raig C, Hurlimann E, Biskup J, Philpot C, Lier H, Engelmann F, Pantaleo A, Cogoli A, Pippia P, Layer LE, Thiel CS, Ullrich O. Signal Transduction In Primary Human T Lymphocytes In Altered Gravity During Parabolic Flight And Clinostat Experiments. *Cell Physiol Biochem.* 2015;35:1034–51. doi: 10.1159/000373930. [[DOI](#)] [[PubMed](#)] [[Google Scholar](#)]

80. Taylor GR, Dardano JR. Human Cellular Immune Responsiveness Following Space Flight. *Aviat Space Environ Med.* 1983;54:S55–9. [[PubMed](#)] [[Google Scholar](#)]

81. Taylor GR, Neale LS, Dardano JR. Immunological Analyses Of U.S. Space Shuttle Crewmembers. *Aviat Space Environ Med.* 1986;57:213–7. [[PubMed](#)] [[Google Scholar](#)]

82. Tonegawa S. Somatic Generation Of Antibody Diversity. *Nature.* 1983;302:575–81. doi: 10.1038/302575a0. [[DOI](#)] [[PubMed](#)] [[Google Scholar](#)]

83. Tschumper RC, Asmann YW, Hossain A, Huddleston PM, Wu X, Dispenzieri A, Eckloff BW, Jelinek DF. Comprehensive Assessment Of Potential Multiple Myeloma Immunoglobulin Heavy Chain V-D-J Intracлонаl Variation Using Massively Parallel Pyrosequencing. *Oncotarget.* 2012;3:502–13. doi: 10.18632/oncotarget.469. [[DOI](#)] [[PMC free article](#)] [[PubMed](#)] [[Google Scholar](#)]

84. Voss EW., Jr Prolonged Weightlessness And Humoral Immunity. *Science.* 1984;225:214–5. doi: 10.1126/science.6729476. [[DOI](#)] [[PubMed](#)] [[Google Scholar](#)]

85. Wardemann HBCE. Novel Approaches To Analyze Immunoglobulin Repertoires. *Trends In Immunology.* 2017;38:471–482. doi: 10.1016/j.it.2017.05.003. [[DOI](#)] [[PubMed](#)] [[Google Scholar](#)]

86. Wei LX, Zhou JN, Roberts AI, Shi YF. Lymphocyte Reduction Induced By Hindlimb Unloading: Distinct Mechanisms In The Spleen And Thymus. *Cell Res.* 2003;13:465–71. doi: 10.1038/sj.cr.7290189. [[DOI](#)] [[PubMed](#)] [[Google Scholar](#)]

87. Xu JL, Davis MM. Diversity In The Cdr3 Region Of V(H) Is Sufficient For Most Antibody Specificities. *Immunity*. 2000;13:37–45. doi: 10.1016/s1074-7613(00)00006-6. [[DOI](#)] [[PubMed](#)] [[Google Scholar](#)]
88. Yang Y, Wang C, Yang Q, Kantor AB, Chu H, Ghosn EE, Qin G, Mazmanian SK, Han J, Herzenberg LA. Distinct Mechanisms Define Murine B Cell Lineage Immunoglobulin Heavy Chain (Igh) Repertoires. *Elife*. 2015;4:E09083. doi: 10.7554/eLife.09083. [[DOI](#)] [[PMC free article](#)] [[PubMed](#)] [[Google Scholar](#)]
89. Zuckerman NS, Howard WA, Bismuth J, Gibson K, Edelman H, Berrih-Aknin S, Dunn-Walters D, Mehr R. Ectopic Gc In The Thymus Of Myasthenia Gravis Patients Show Characteristics Of Normal Gc. *Eur J Immunol*. 2010;40:1150–61. doi: 10.1002/eji.200939914. [[DOI](#)] [[PubMed](#)] [[Google Scholar](#)]

Associated Data

This section collects any data citations, data availability statements, or supplementary materials included in this article.

Supplementary Materials

1

[NIHMS928411-supplement-1.xml](#) (410B, xml)

2

[NIHMS928411-supplement-2.pdf](#) (954.1KB, pdf)

3

[NIHMS928411-supplement-3.pdf](#) (229KB, pdf)

4

[NIHMS928411-supplement-4.tif](#) (3.4MB, tif)

5

[NIHMS928411-supplement-5.pdf](#) (82.9KB, pdf)